

Advanced Beam Instrumentation and Diagnostics for FELs

P. Evtushenko, *Jefferson Lab*

with help and insights from many others:

S. Benson, D. Douglas, *Jefferson Lab*

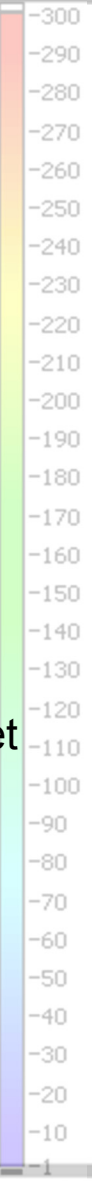
T. Maxwell, P. Krejcik, *SLAC*

S. Wesch, *now at BESSY*

E. Hass, B. Schmidt, *DESY*

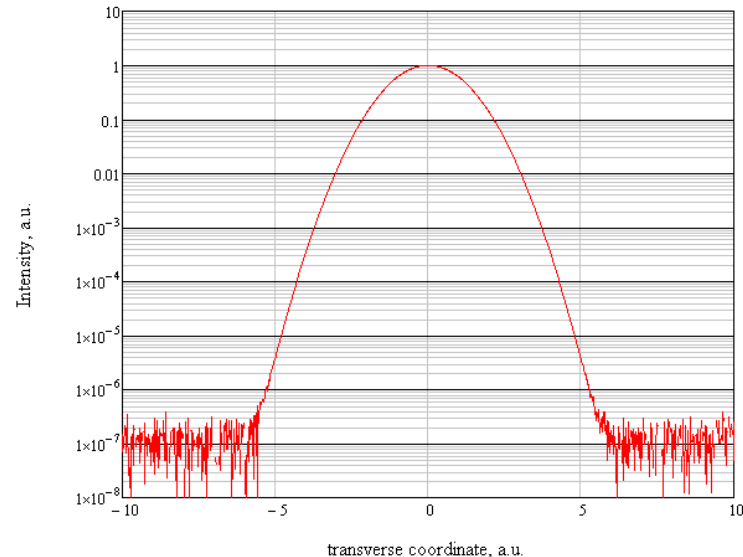
High current (10mA) operation experience

- ❖ Operation of JLab FEL with high average current requires a compromise (in terms of match) between high peak beam brightness (required by FEL) and very low beam loss
- ❖ The match is iterative process and often does not converge easily
- ❖ For the transverse beam profile measurements and transverse match JLab FEL relies heavily on beam imaging (2D distribution); very large number of beam viewers
- ❖ LINAC beams have neither the time nor the mechanism to come to equilibrium (*unlike storage rings, which also run high current*)
- ❖ Note, when setting up a high current accelerators with tune-up beam, beam halo is something *invisible* (due to the dynamic range of the measurements) during the setup, yet causing a lot of difficulties when trying to run high current
- ❖ **Increase the DR significantly to make the halo measurable visible with tune-up beam already; measure the phase space distribution with the LDR and use such information for the match. When DR is large enough no need to separate what is core and what is halo.**



LDR imaging components

- ❖ Involved in any beam imaging technique: **source, optics, sensor(s)**
- ❖ One of the issues is the DR of sensors (**500 .. 1000**). Limited by Q.E. of Si at optical wavelength and thermal noise. One possibility to use **2 or 3 sensors with different effective gain simultaneously** and to combine data in one LDR image digitally.
- ❖ High current LINACs are setup with tune-up beam – much reduced beam current and power; **amount of charge (and photons)** for measurements has certain **limit**
- ❖ From experience (calculations tested by experiments) we know the **safe level of beam current/power** for a low duty cycle (tune-up) beam
- ❖ For example (JLab FEL) typical beam size of hundred μm . OTR signal is attenuated by ~ 10 to keep CCD from saturation. For YAG:Ce viewers attenuation of at least 100 is used.
- ❖ Using OTR there is enough intensity to measure **4 upper decades**; lower two decades need gain of about **100** to be measured.
- ❖ **The key elements:**
 - **alignment and linearity**
 - **image intensifiers**
 - **combining algorithm(s)**
 - **CCD saturation**

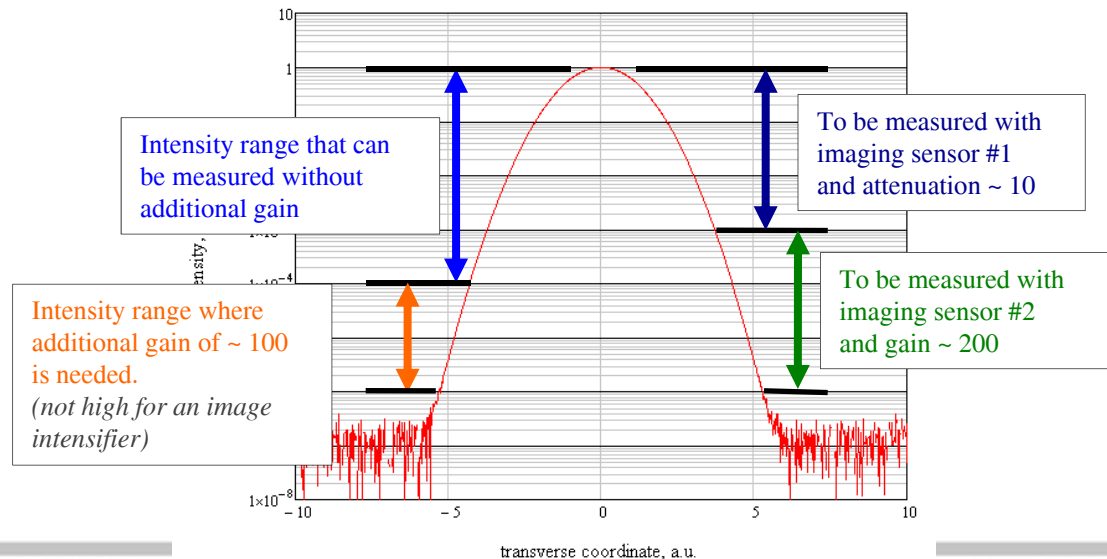


LDR imaging components

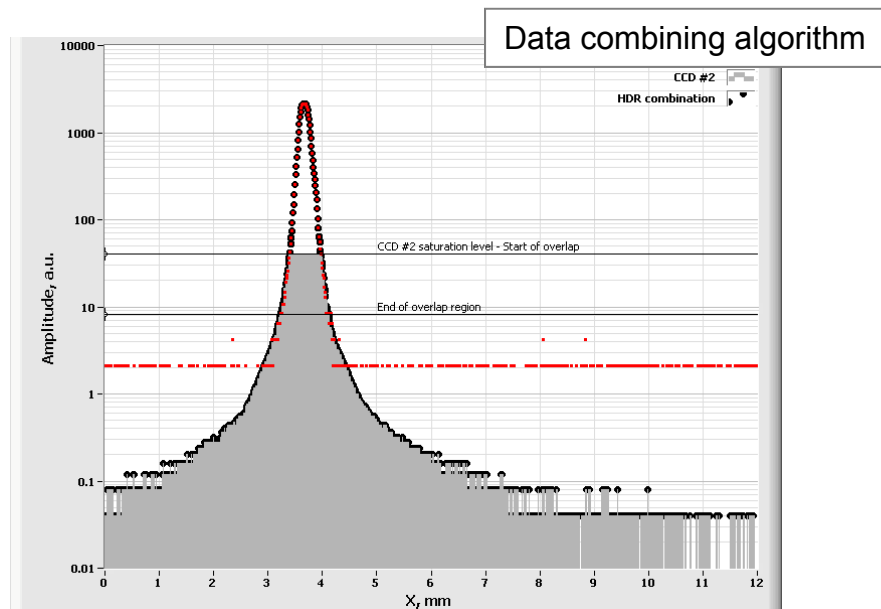
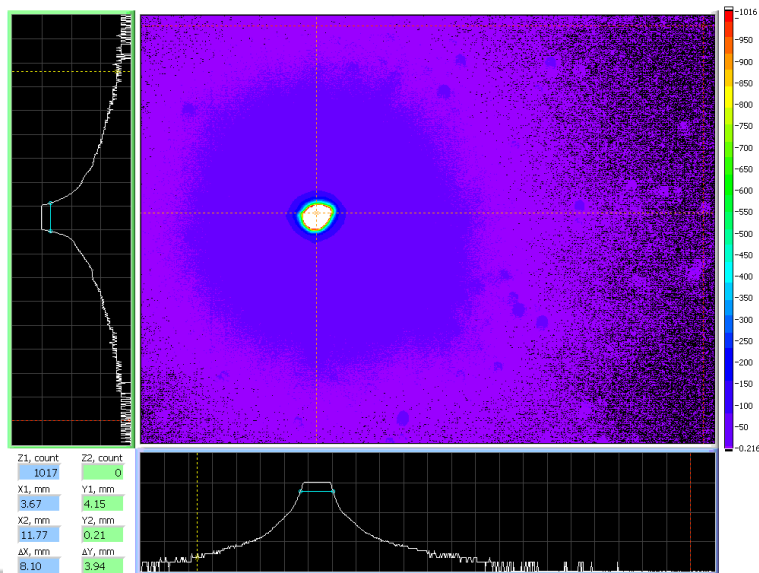
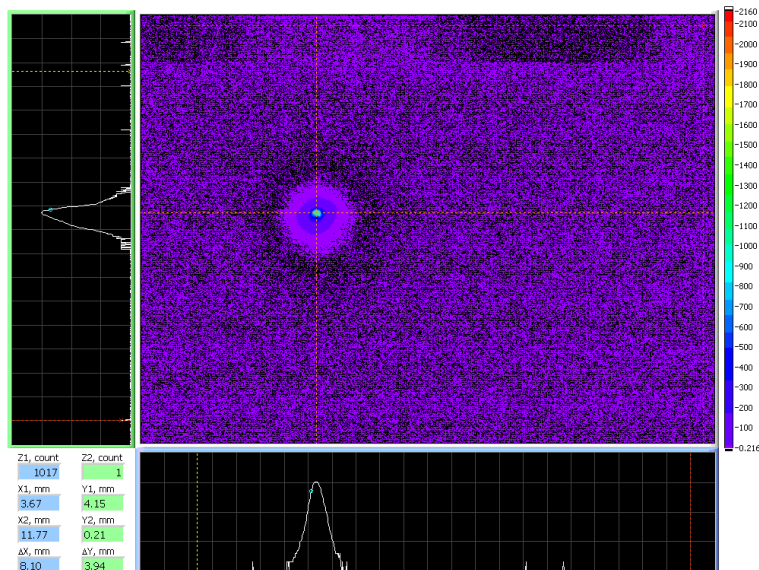
- ❖ Involved in any beam imaging technique: **source, optics, sensor(s)**
- ❖ One of the issues is the DR of sensors (**500 .. 1000**). Limited by Q.E. of Si at optical wavelength and thermal noise. One possibility to use **2 or 3 sensors with different effective gain simultaneously** and to combine data in one LDR image digitally.
- ❖ High current LINACs are setup with tune-up beam – much reduced beam current and power; **amount of charge (and photons)** for measurements has certain **limit**
- ❖ From experience (calculations tested by experiments) we know the **safe level of beam current/power** for a low duty cycle (tune-up) beam
- ❖ For example (JLab FEL) typical beam size of hundred μm . OTR signal is attenuated by ~ 10 to keep CCD from saturation. For YAG:Ce viewers attenuation of at least 100 is used.
- ❖ Using OTR there is enough intensity to measure **4 upper decades**; lower two decades need gain of about **100** to be measured.

- ❖ **The key elements:**

- **alignment and linearity**
- **image intensifiers**
- **combining algorithm(s)**
- **CCD saturation**

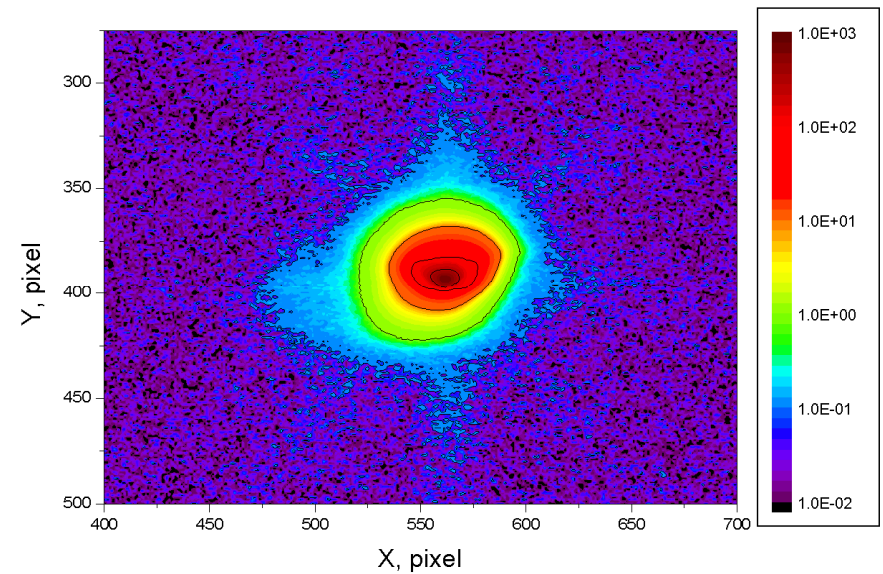
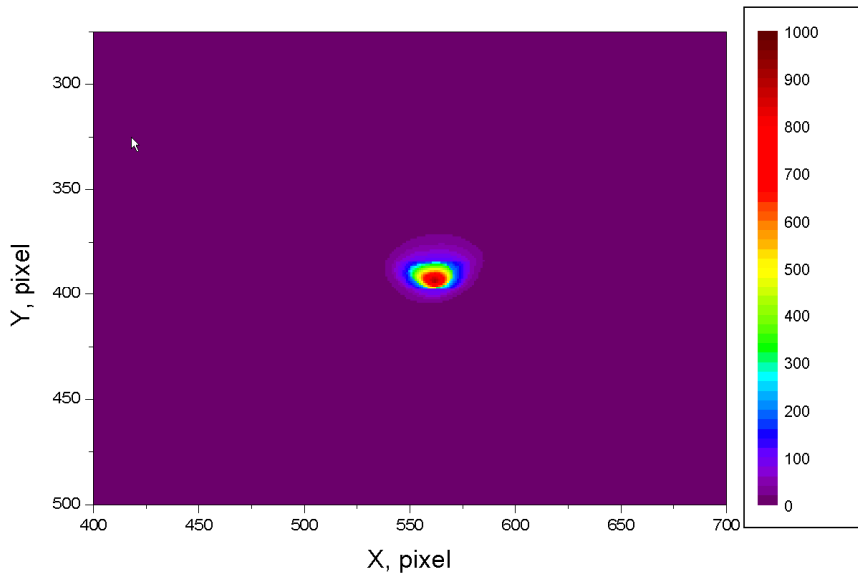


Raw images and combining algorithm



- ❖ Two images (on the left) measured simultaneously with integration times 20 us and 400 us
- ❖ Background measurements and subtraction is crucial! Made separately for two sensors and subtracted on-line.
- ❖ Combining algorithm is efficient enough to provide 5 Hz rep. rate for 1024x768 images
- ❖ At the time of measurements was limited by the flexibility of DLPC
- ❖ Demonstrated dynamic range of $\sim 5E+4$ (factor of 100 increase)
- ❖ Integration time is used for normalization and overlap (sufficient)
- ❖ Averaging also improves SNR and therefore DR (beam stability)

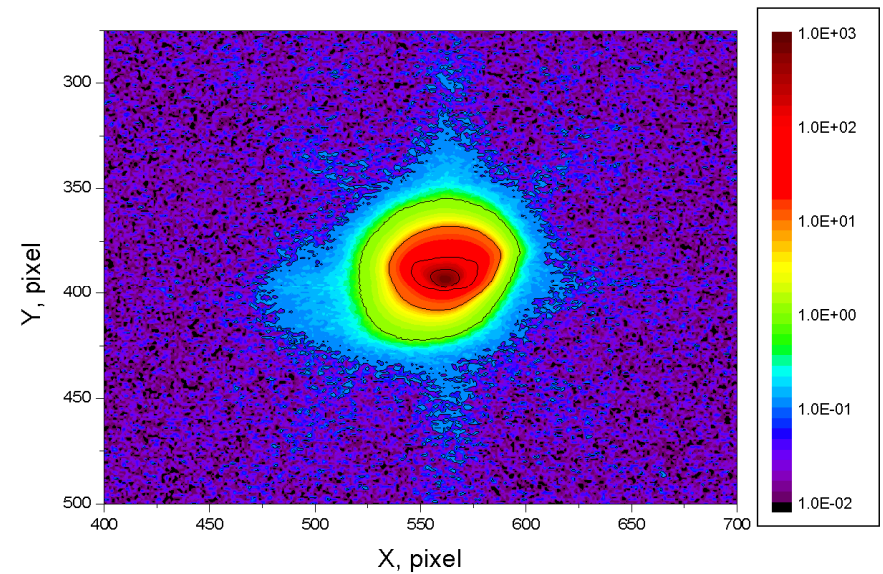
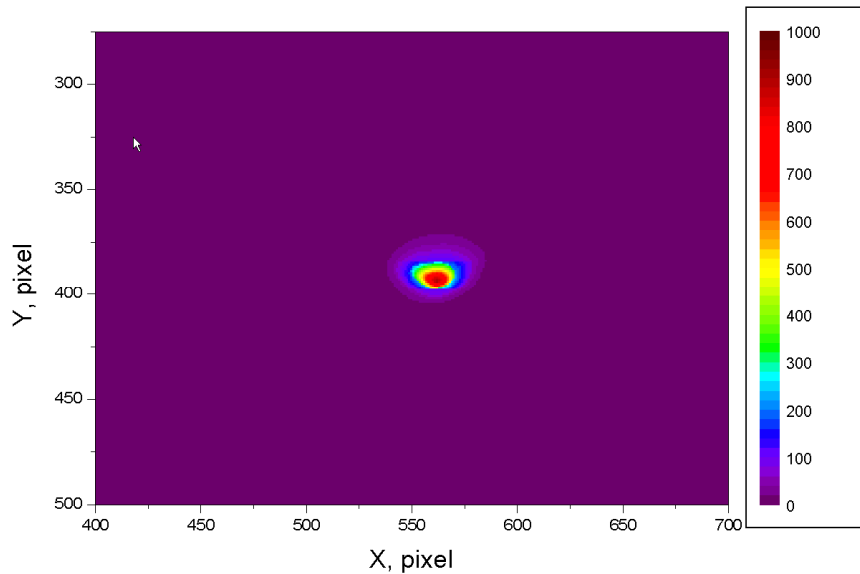
linear & log; the “trouble” with the RMS



- ❖ The two images show exactly the same data (beam profile - (x,y)) but in linear and log scale
- ❖ Next step is to use such measurements for beam characterization, emittance and Twiss parameters measurements (add x' and y')
- ❖ Ultimately tomographic measurements are planned; but first just quad scan

$$w_{RMS}^X = \int x^2 f(x) dx$$

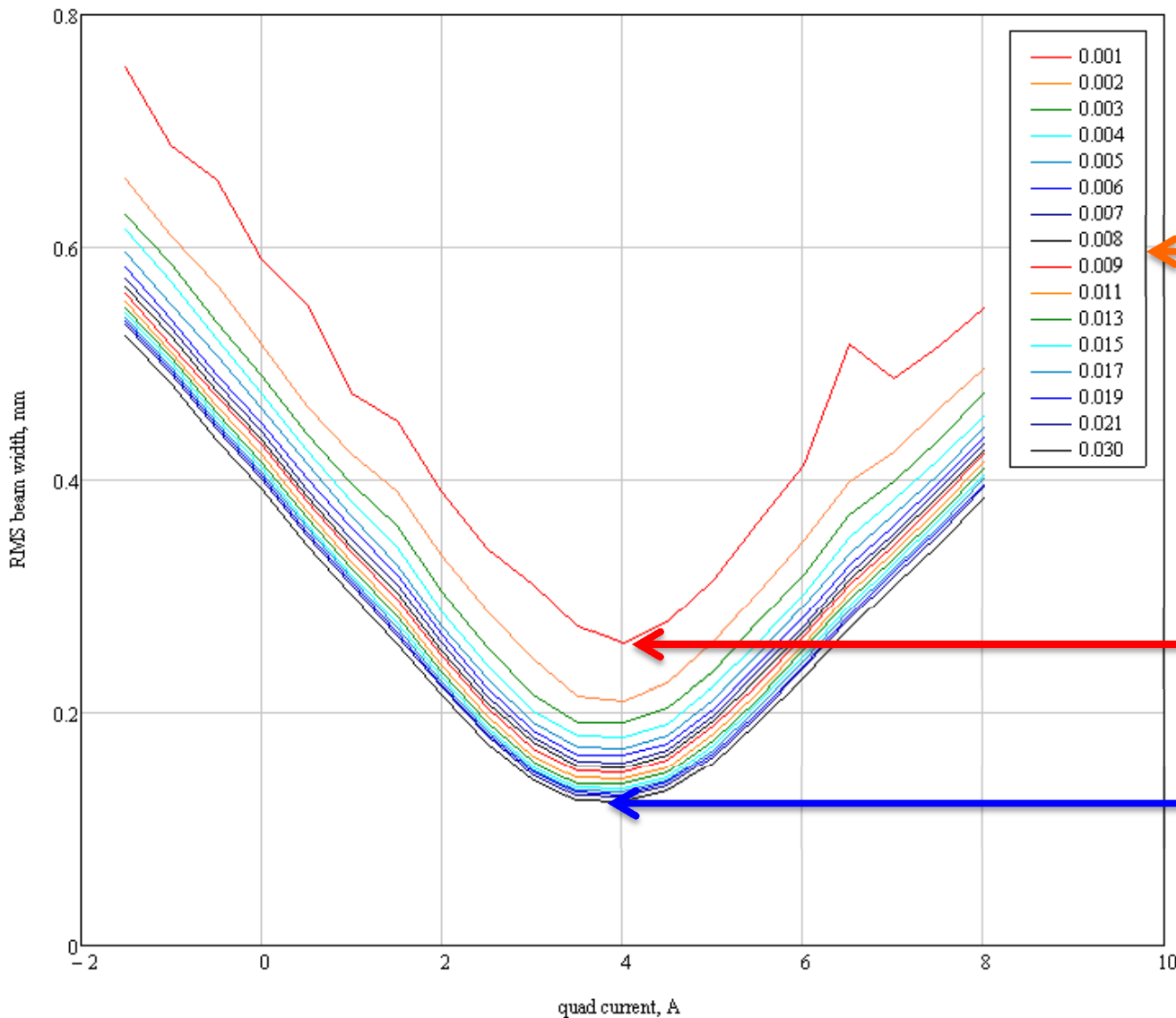
linear & log; the “trouble” with the RMS



- ❖ The two images show exactly the same data (beam profile - (x,y)) but in linear and log scale
- ❖ Next step is to use such measurements for beam characterization, emittance and Twiss parameters measurements (add x' and y')
- ❖ Ultimately tomographic measurements are planned; but first just quad scan
- ❖ For **non-Gaussian beam** RMS beam width is a tricky thing!
It depends on how much of *tails* of the distribution function $f(x)$ is taken in to account.

$$w_{RMS}^X = \int x^2 f(x) dx$$

Quadrupole scan raw data

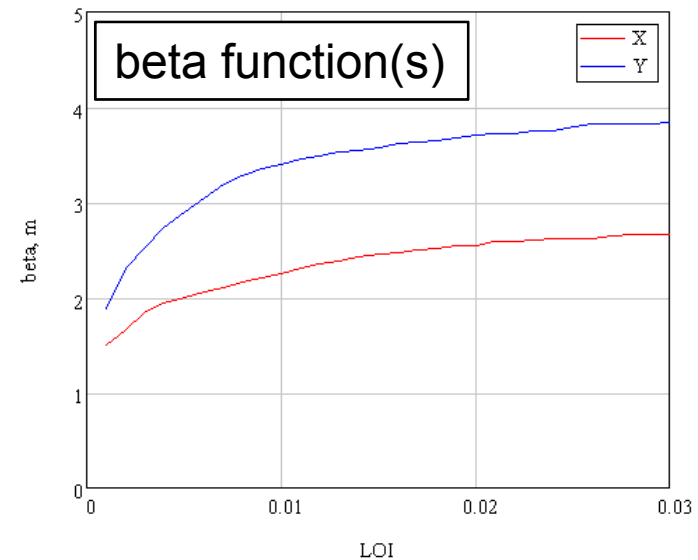
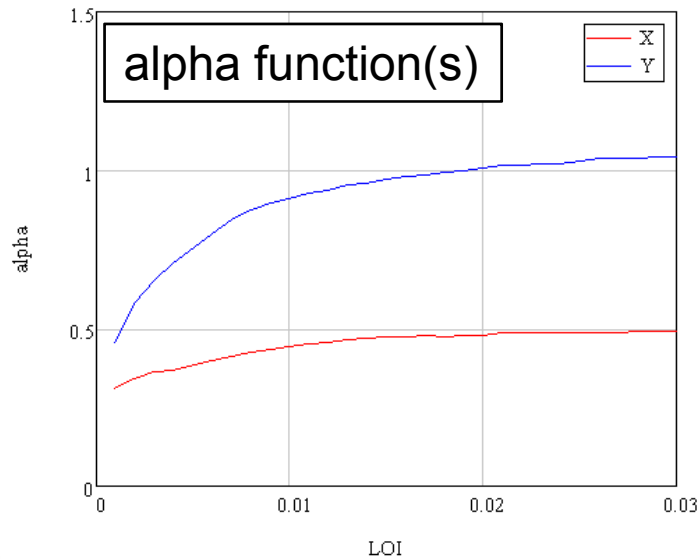
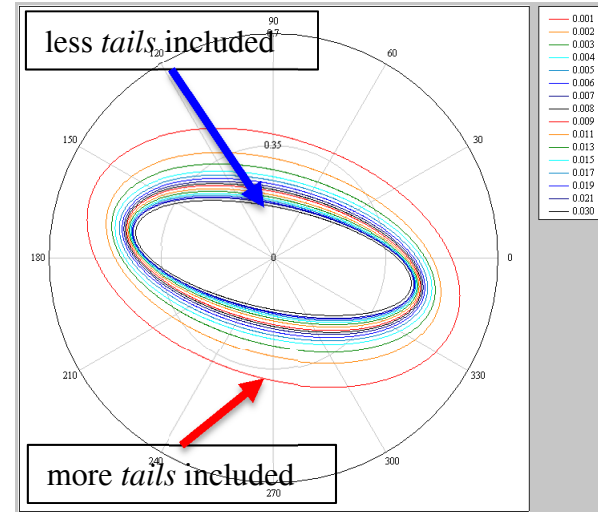
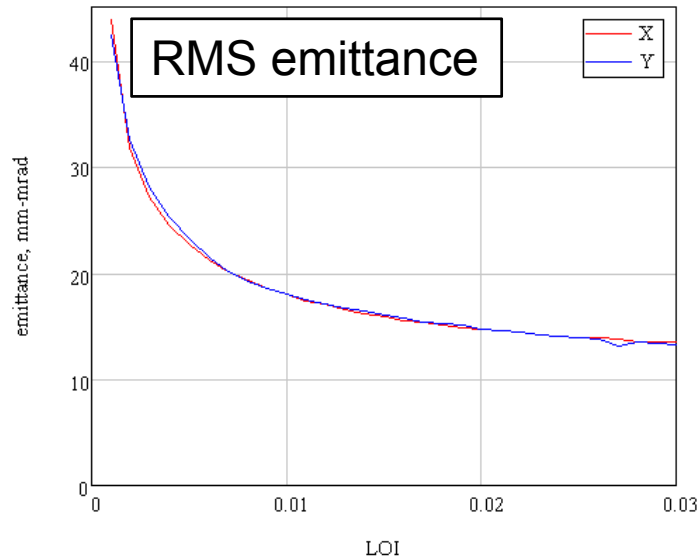


Level of interest (LOI)

more *tails* included

less *tails* included

Emittance and Twiss parameters

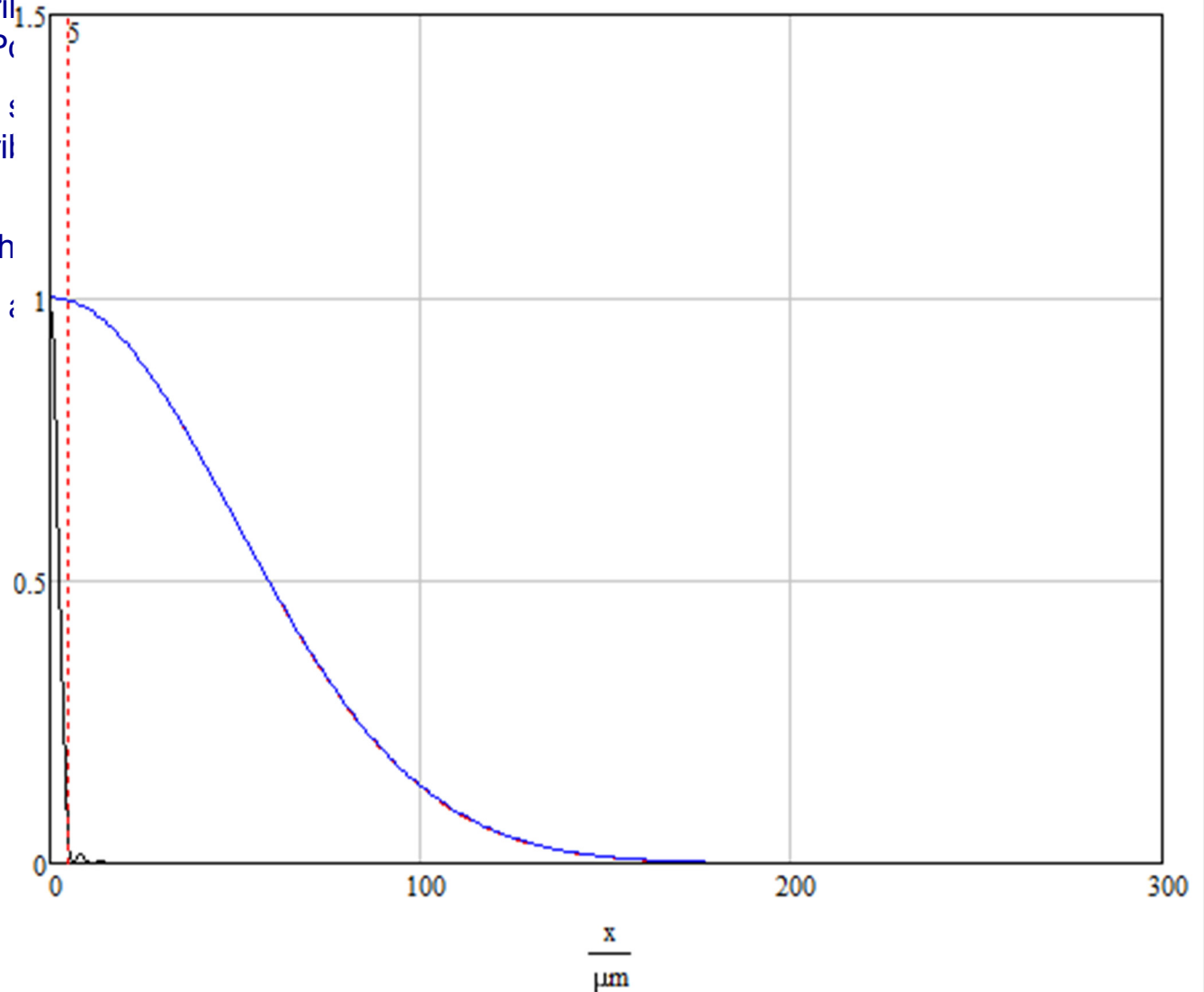


Diffraction limit and PSF

- ❖ Imaging → measured distribution is a convolution of source distribution and so-called Point Spread Function (PSF)
- ❖ PFS determined by optical system angular acceptance but also by the source angular distribution. Different beam viewers have different PSF.
- ❖ **Diffraction** determines rather hard limits to the DR
- ❖ Ways to mitigate: increase angular acceptance, use spatial filter, coronagraph-like optics

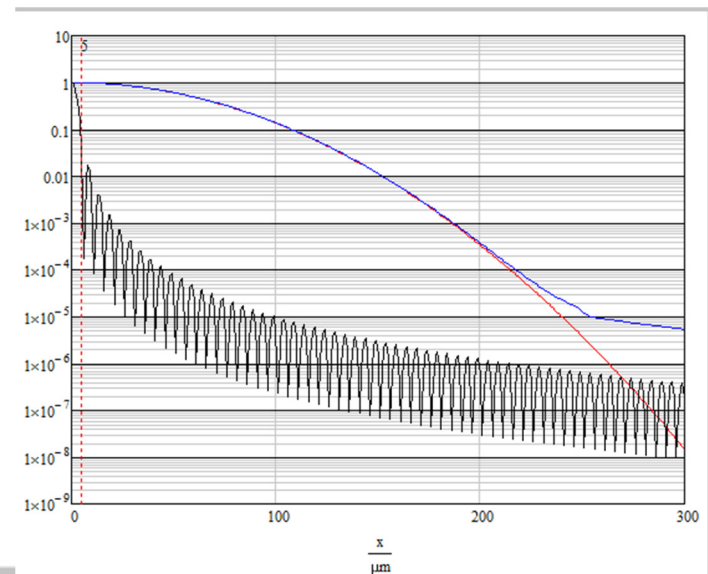
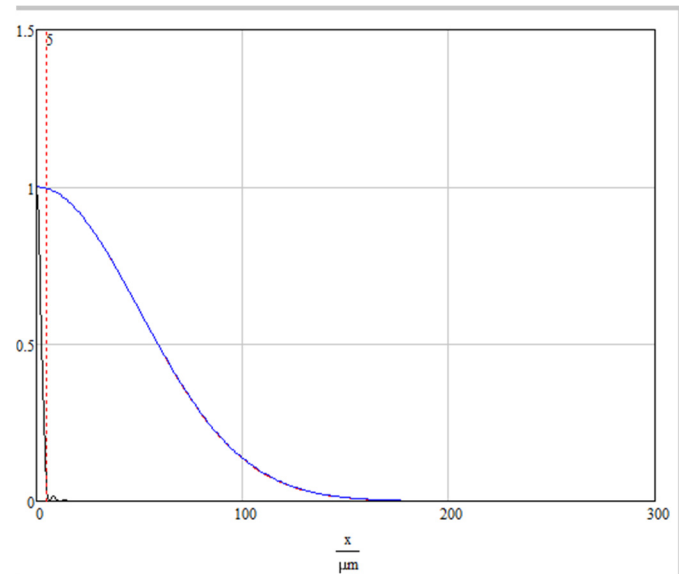
Diffraction limit and PSF

- ❖ Imaging → measured distribution and so-called PSF
- ❖ PSF determined by optical system by the source angular distribution different PSF.
- ❖ **Diffraction** determines rather
- ❖ Ways to mitigate: increase source size, coronagraph-like optics



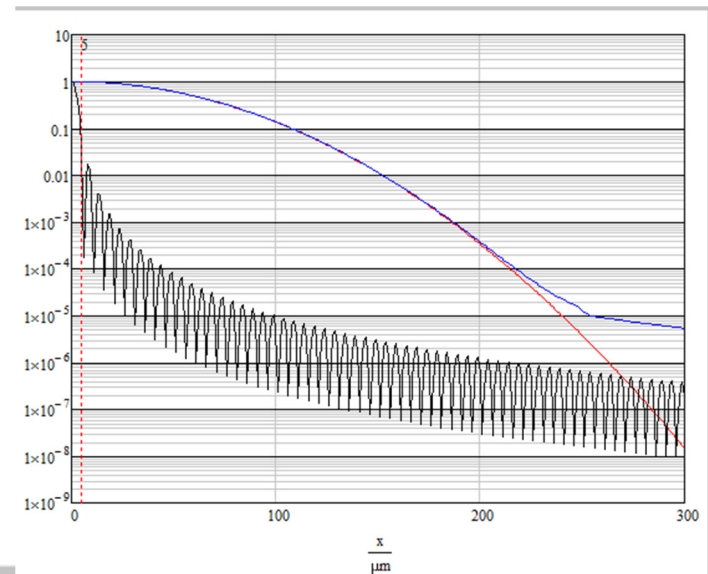
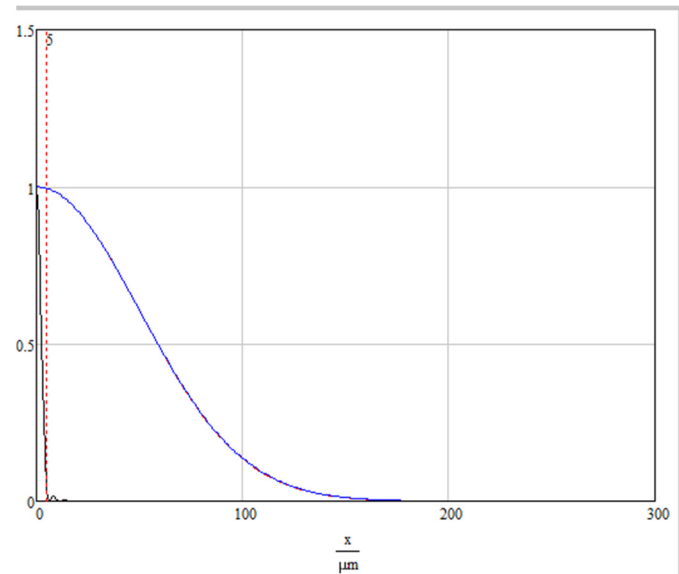
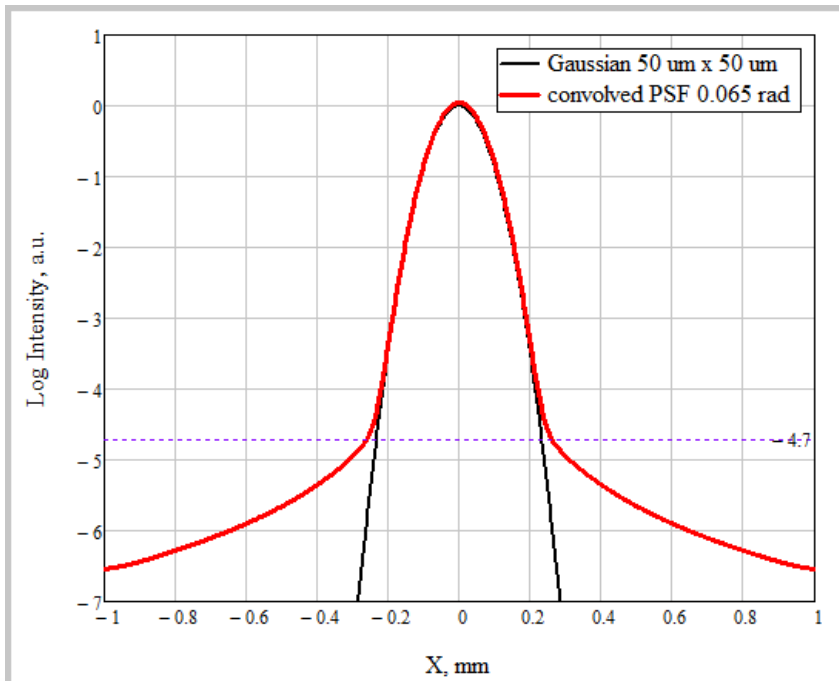
Diffraction limit and PSF

- ❖ Imaging → measured distribution is a convolution of source distribution and so-called Point Spread Function (PSF)
- ❖ PFS determined by optical system angular acceptance but also by the source angular distribution. Different beam viewers have different PSF.
- ❖ **Diffraction** determines rather hard limits to the DR
- ❖ Ways to mitigate: increase angular acceptance, use spatial filter, coronagraph-like optics



Diffraction limit and PSF

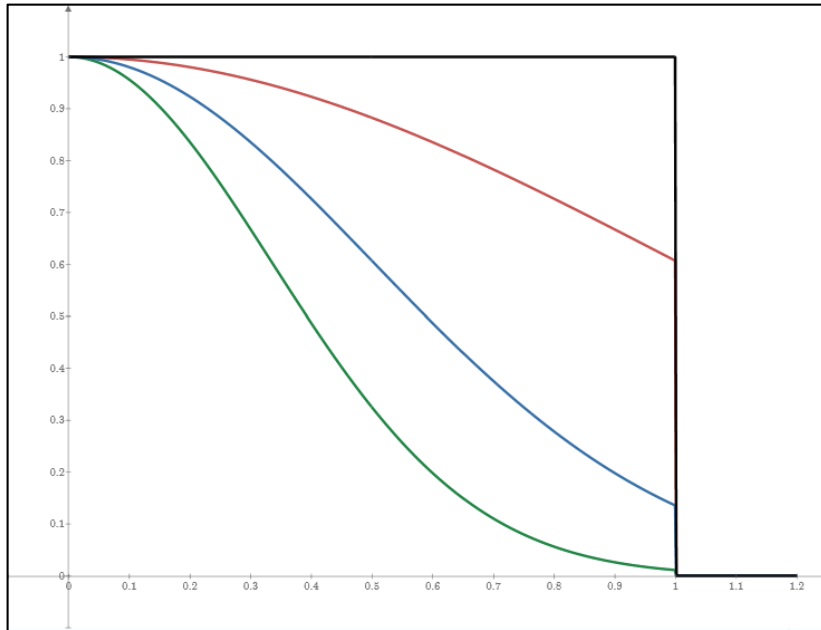
- ❖ Imaging → measured distribution is a convolution of source distribution and so-called Point Spread Function (PSF)
- ❖ PFS determined by optical system angular acceptance but also by the source angular distribution. Different beam viewers have different PSF.
- ❖ **Diffraction** determines rather hard limits to the DR
- ❖ Ways to mitigate: increase angular acceptance, use spatial filter, coronagraph-like optics



Objective lens pupil apodization

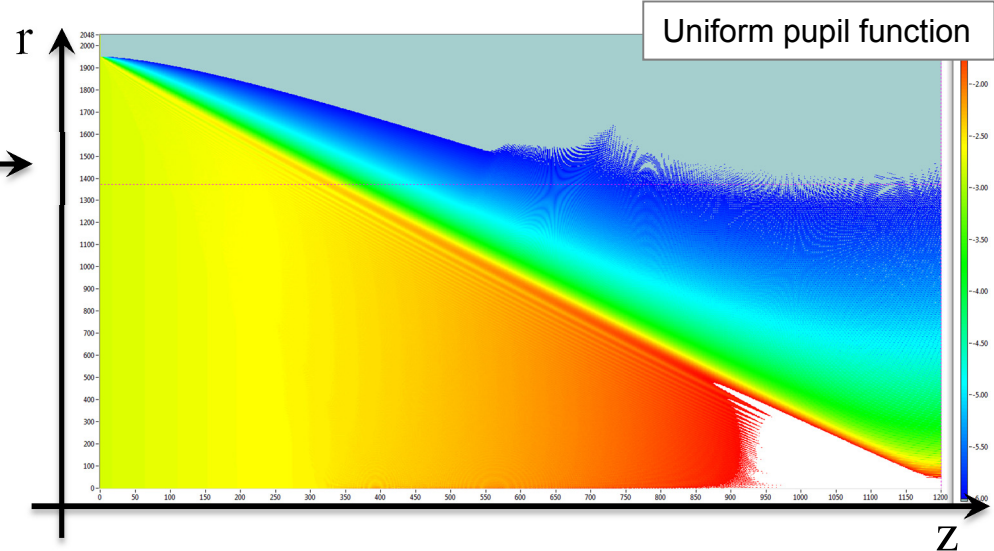
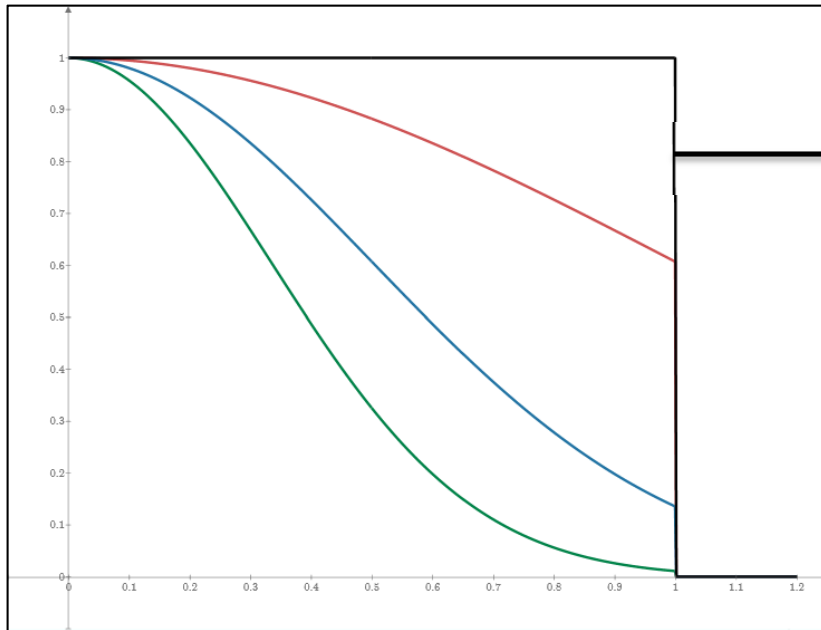
- ❖ First a Lyot's coronagraph was considered to improve the PSF, but this would not allow for simultaneous measurements of the beam core and halo, but it is a good exercise
- ❖ *Domain of Fourier optic, always Fresnel approximation – numerical calculations required for most of the interesting cases – becomes demanding on CPU and memory quickly due to large apertures and optical wavelength ($\sim 0.5 \mu\text{m}$)*
- ❖ Implemented and used quasi-discrete Hankel transform for optics modeling (allows to do 1D calculations vs. 2D)
- ❖ Fourier optics \rightarrow image plane = Fourier transform of pupil function for a point source (this is the PSF)
- ❖ Then it is easy to see that the uniform pupil function, i.e., the hard lens edge is the problem (*besides the uncertainty principle, which also adds to the problem*)
- ❖ Apodization – modification of the pupil function; First considered Gaussian amplitude apodization

Objective lens pupil apodization



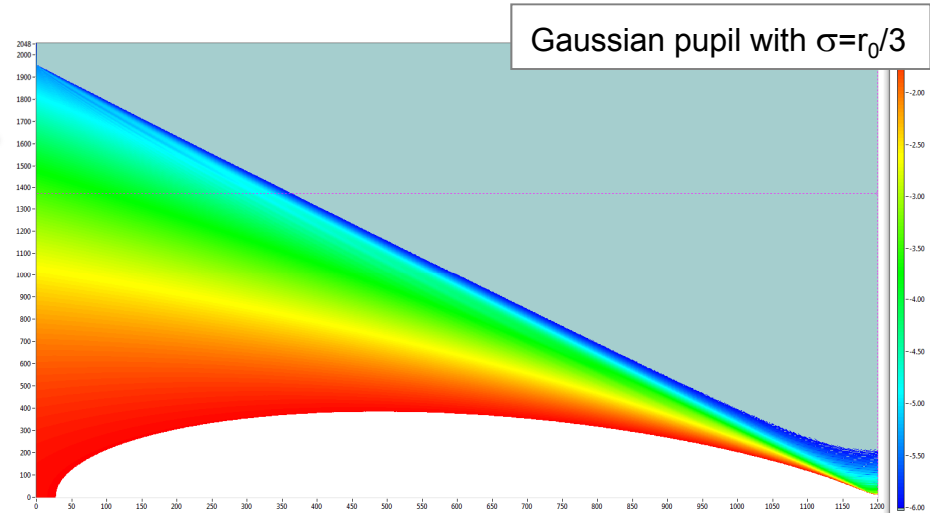
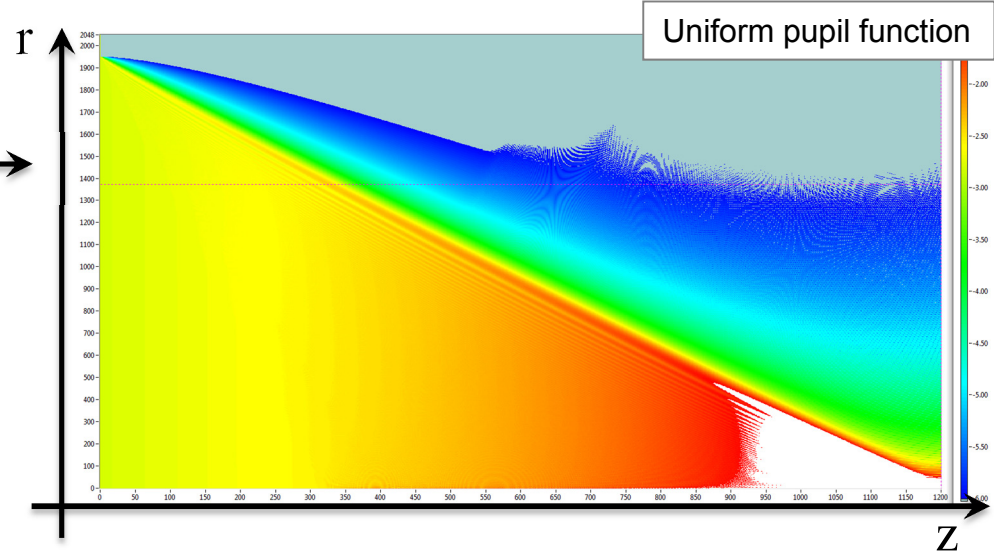
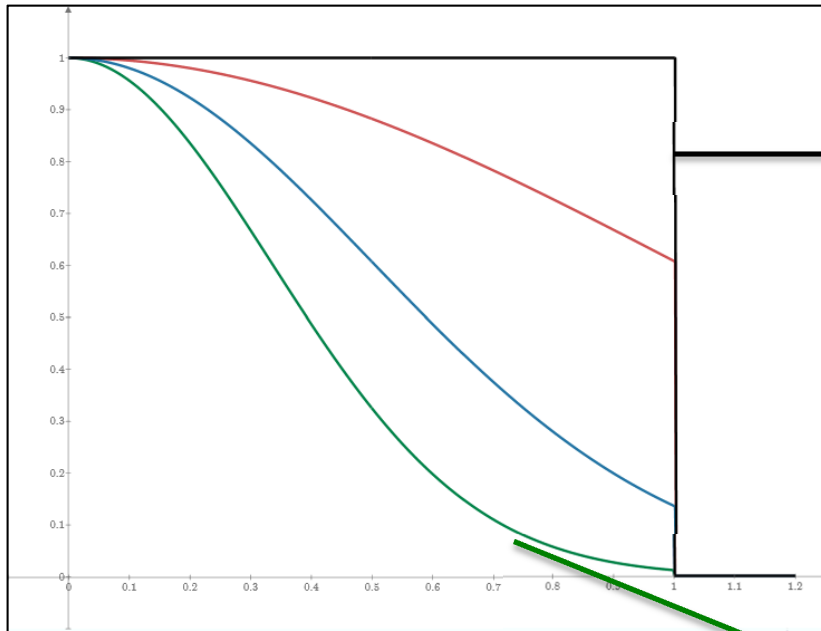
- ❖ Fourier optics → image plane = Fourier transform of pupil function for a point source (this is the PSF)
- ❖ Then it is easy to see that the uniform pupil function, i.e., the hard lens edge is the problem (*besides the uncertainty principal, which also adds to the problem*)
- ❖ Apodization – modification of the pupil function; First considered Gaussian amplitude apodization

Objective lens pupil apodization



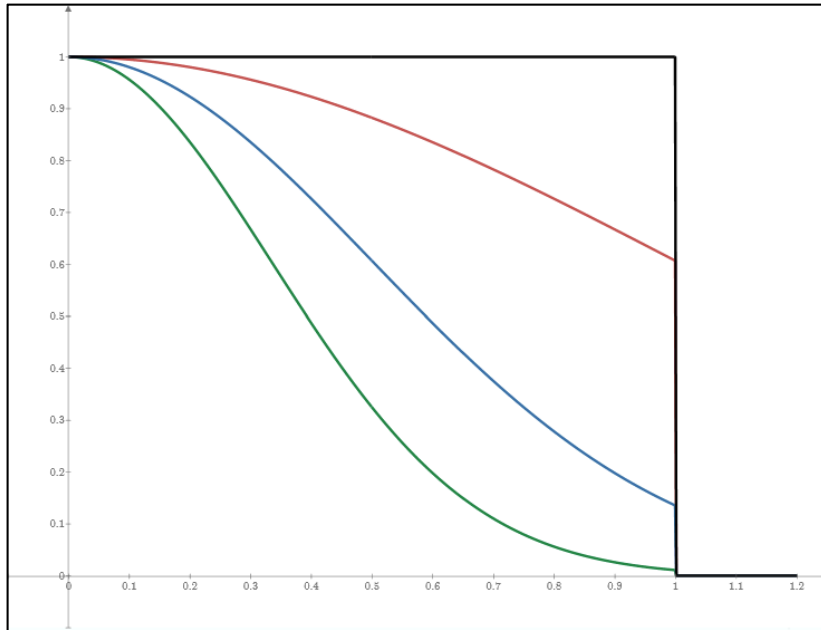
- ❖ Fourier optics \rightarrow image plane = Fourier transform of pupil function for a point source (this is the PSF)
- ❖ Then it is easy to see that the uniform pupil function, i.e., the hard lens edge is the problem (*besides the uncertainty principle, which also adds to the problem*)
- ❖ Apodization – modification of the pupil function; First considered Gaussian amplitude apodization

Objective lens pupil apodization

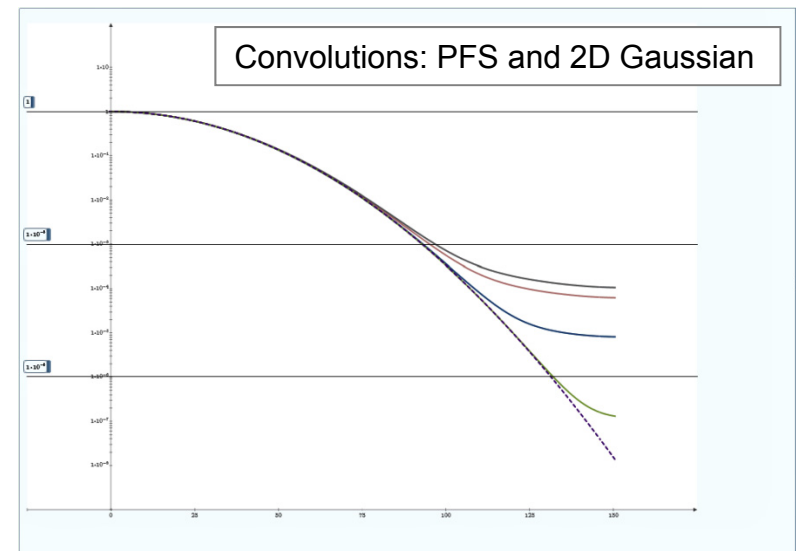
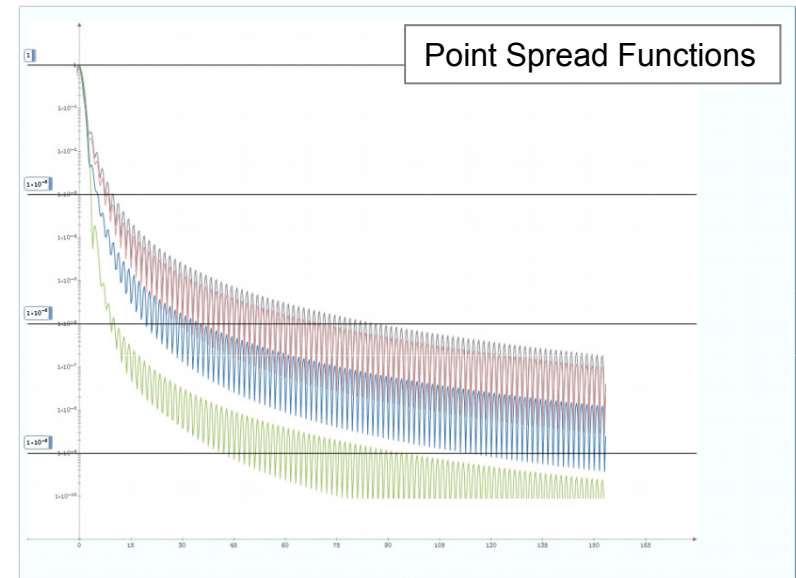


- ❖ Fourier optics \rightarrow image plane = Fourier transform of pupil function for a point source (this is the PSF)
- ❖ Then it is easy to see that the uniform pupil function, i.e., the hard lens edge is the problem (*besides the uncertainty principal, which also adds to the problem*)
- ❖ Apodization – modification of the pupil function; First considered Gaussian amplitude apodization

Objective lens pupil apodization

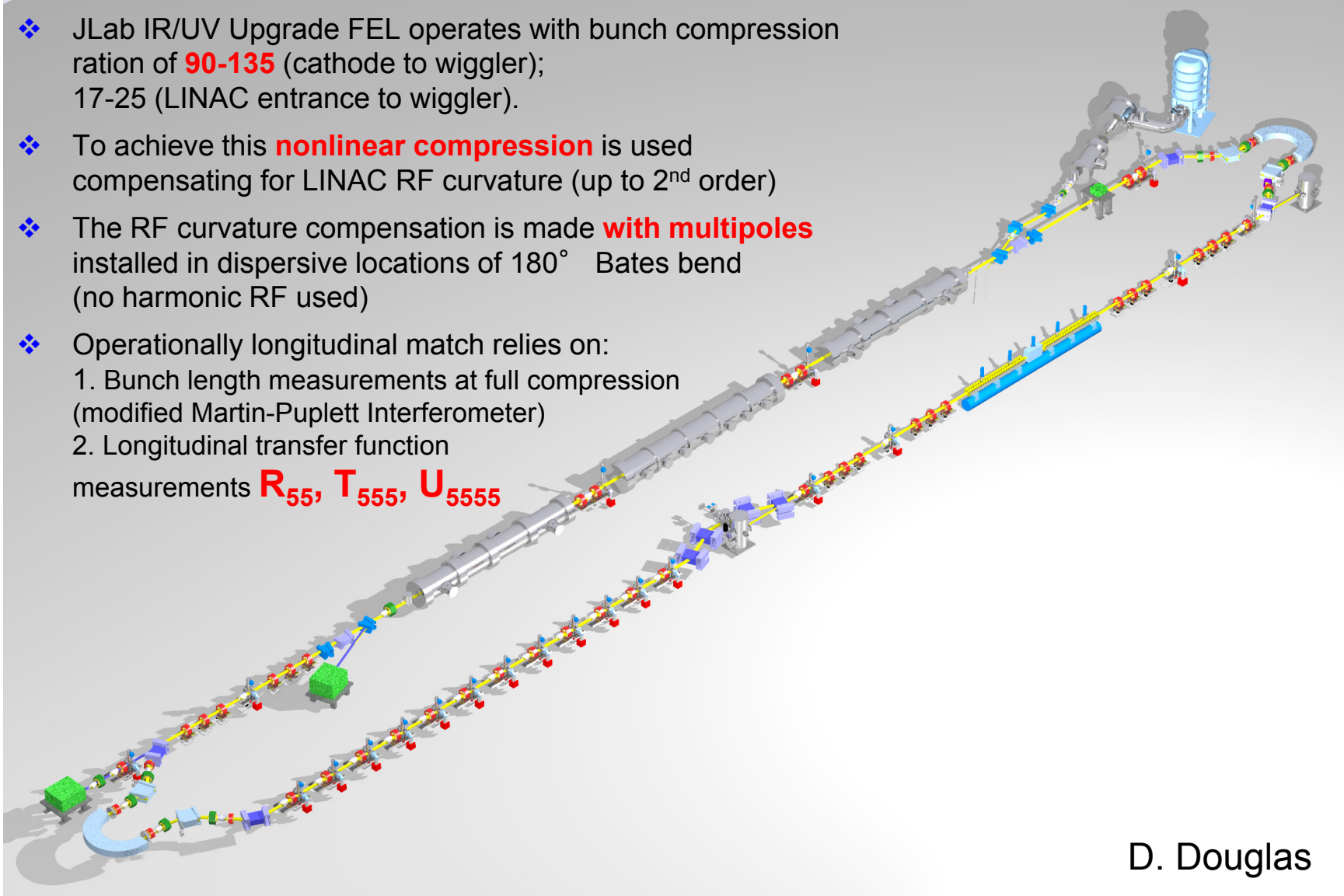


- ❖ Theoretically apodization works well
- ❖ Gaussian is just one of the possibilities, not necessarily the most optimal one
- ❖ The crucial question is how accurately an apodization can be implemented
- ❖ Uniformity of coatings, fluctuations of refraction index - **minimizing overall phase front errors**



Non-linear compression

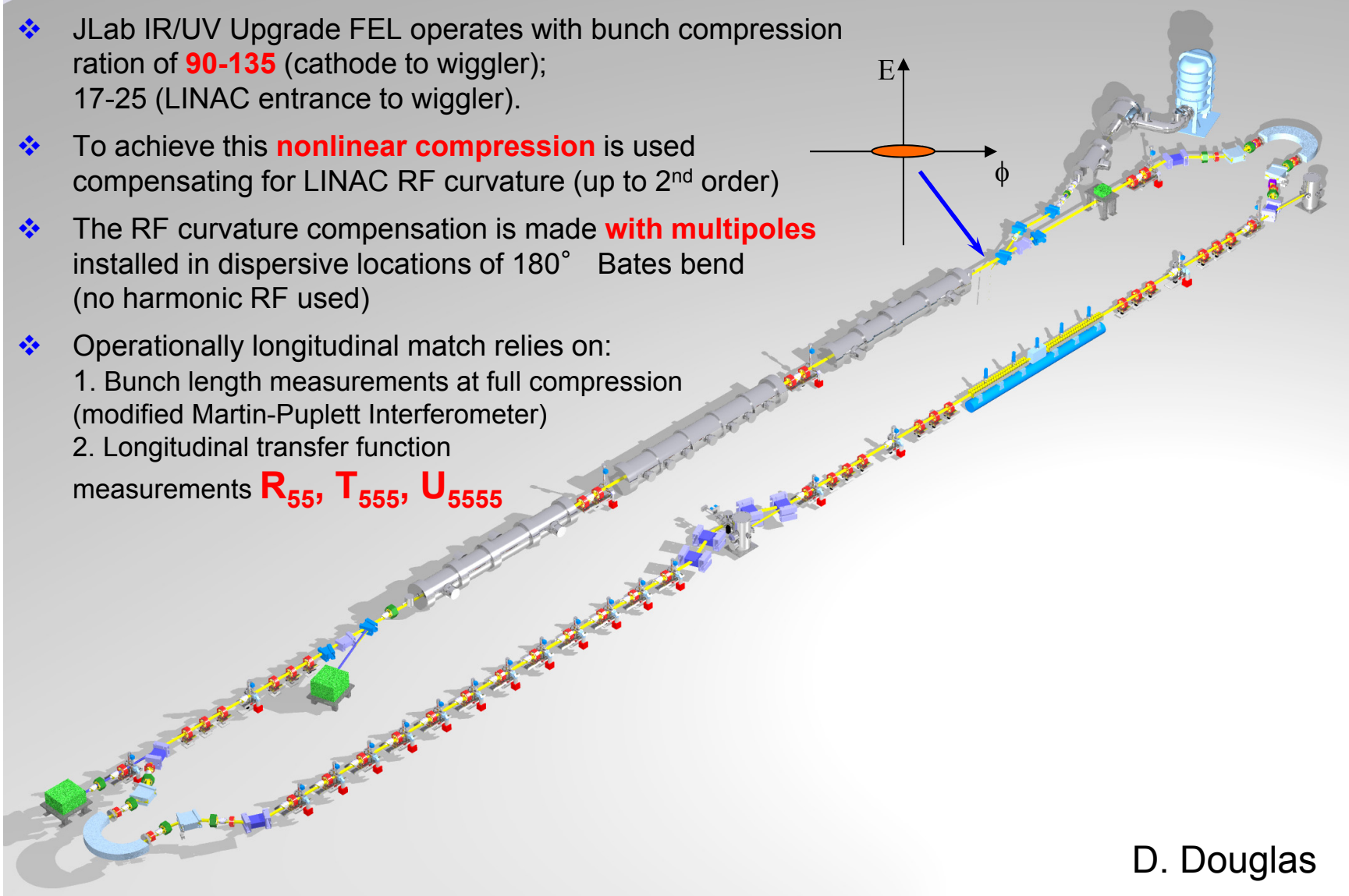
- ❖ JLab IR/UV Upgrade FEL operates with bunch compression ratio of **90-135** (cathode to wiggler); 17-25 (LINAC entrance to wiggler).
- ❖ To achieve this **nonlinear compression** is used compensating for LINAC RF curvature (up to 2nd order)
- ❖ The RF curvature compensation is made **with multipoles** installed in dispersive locations of 180° Bates bend (no harmonic RF used)
- ❖ Operationally longitudinal match relies on:
 1. Bunch length measurements at full compression (modified Martin-Puplett Interferometer)
 2. Longitudinal transfer function measurements **R_{55} , T_{555} , U_{5555}**



D. Douglas

Non-linear compression

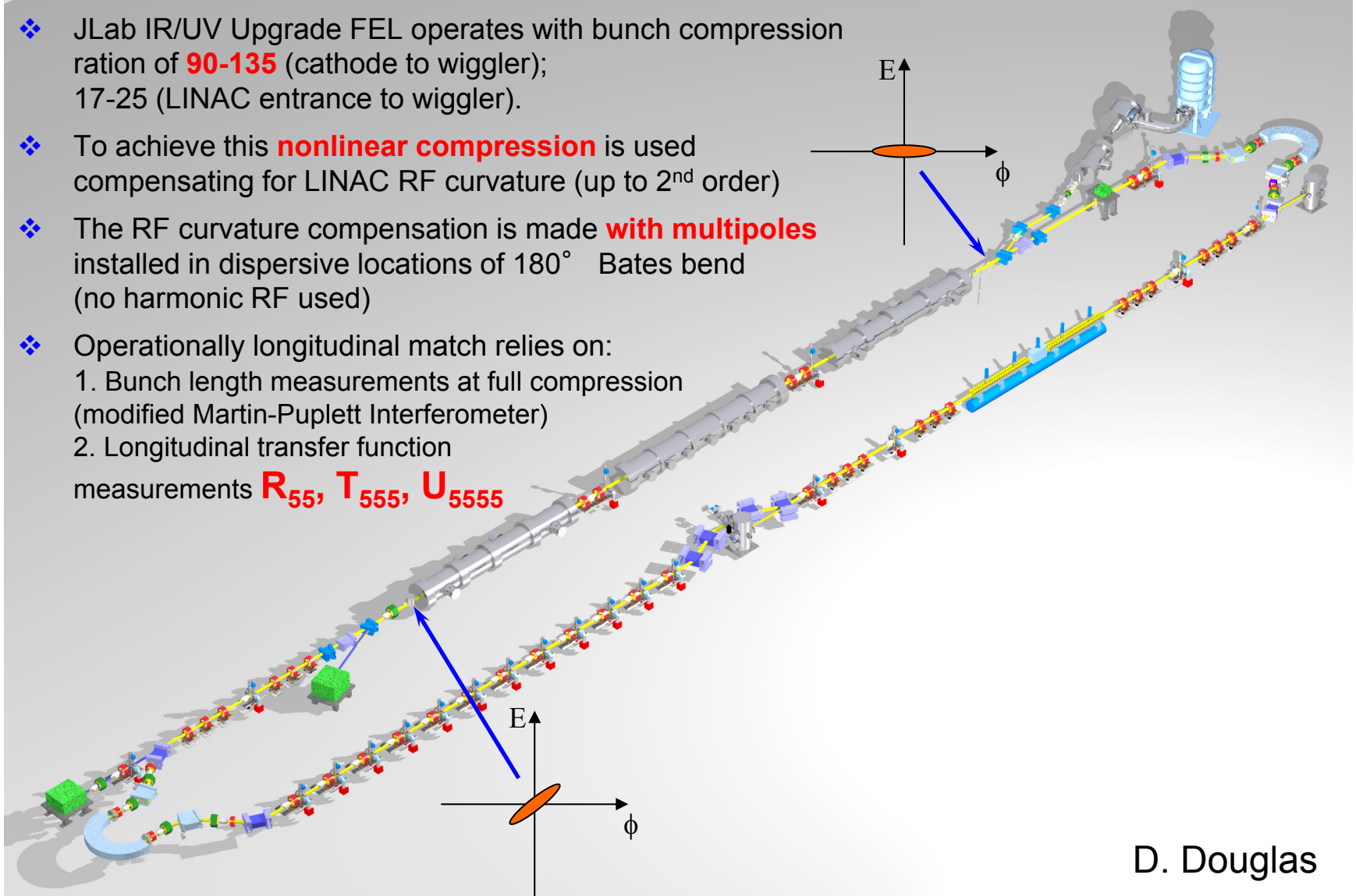
- ❖ JLab IR/UV Upgrade FEL operates with bunch compression ratio of **90-135** (cathode to wiggler); 17-25 (LINAC entrance to wiggler).
- ❖ To achieve this **nonlinear compression** is used compensating for LINAC RF curvature (up to 2nd order)
- ❖ The RF curvature compensation is made **with multipoles** installed in dispersive locations of 180° Bates bend (no harmonic RF used)
- ❖ Operationally longitudinal match relies on:
 1. Bunch length measurements at full compression (modified Martin-Puplett Interferometer)
 2. Longitudinal transfer function measurements **R_{55} , T_{555} , U_{5555}**



D. Douglas

Non-linear compression

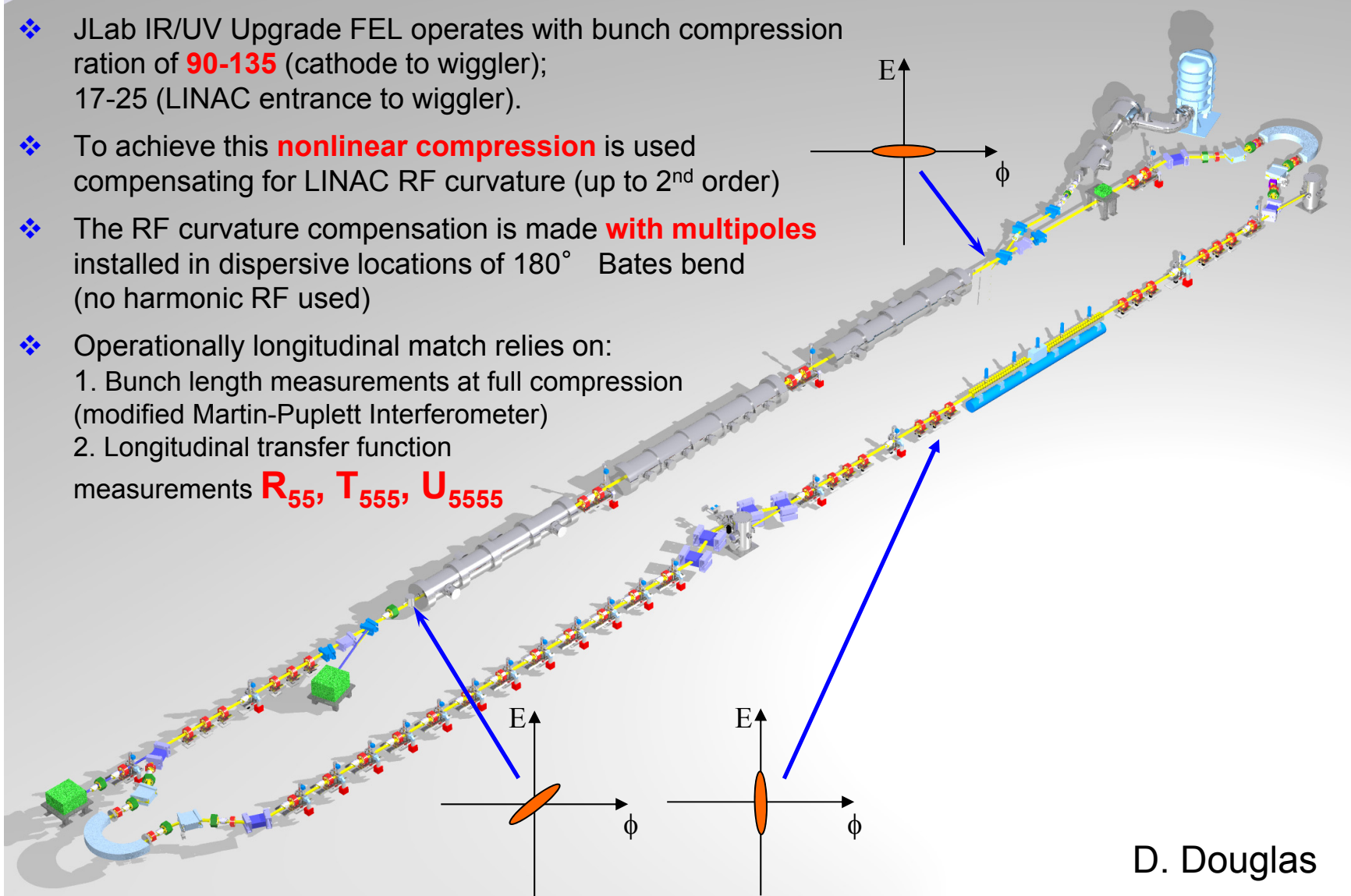
- ❖ JLab IR/UV Upgrade FEL operates with bunch compression ratio of **90-135** (cathode to wiggler); 17-25 (LINAC entrance to wiggler).
- ❖ To achieve this **nonlinear compression** is used compensating for LINAC RF curvature (up to 2nd order)
- ❖ The RF curvature compensation is made **with multipoles** installed in dispersive locations of 180° Bates bend (no harmonic RF used)
- ❖ Operationally longitudinal match relies on:
 1. Bunch length measurements at full compression (modified Martin-Puplett Interferometer)
 2. Longitudinal transfer function measurements **R_{55} , T_{555} , U_{5555}**



D. Douglas

Non-linear compression

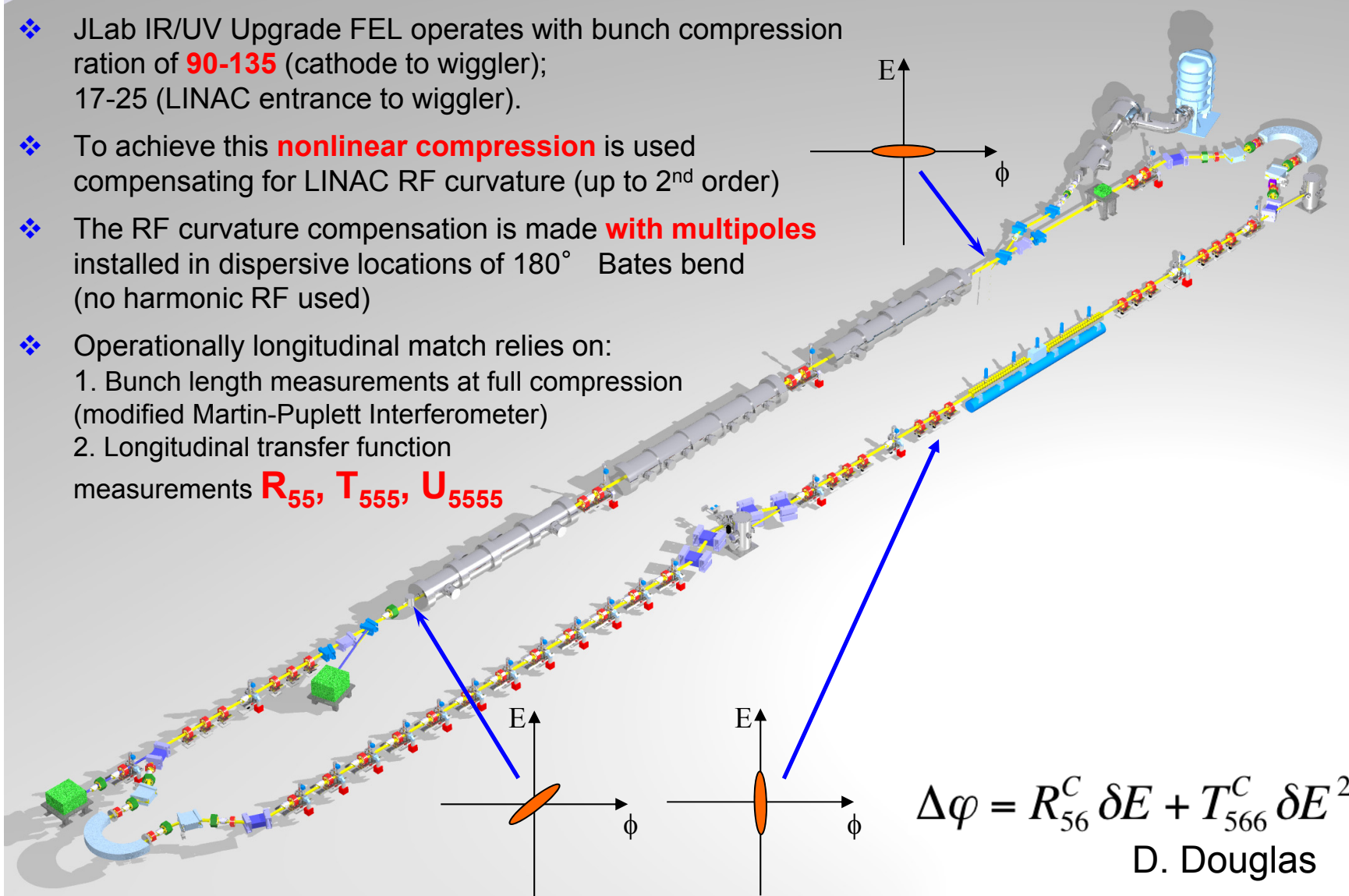
- ❖ JLab IR/UV Upgrade FEL operates with bunch compression ratio of **90-135** (cathode to wiggler); 17-25 (LINAC entrance to wiggler).
- ❖ To achieve this **nonlinear compression** is used compensating for LINAC RF curvature (up to 2nd order)
- ❖ The RF curvature compensation is made **with multipoles** installed in dispersive locations of 180° Bates bend (no harmonic RF used)
- ❖ Operationally longitudinal match relies on:
 1. Bunch length measurements at full compression (modified Martin-Puplett Interferometer)
 2. Longitudinal transfer function measurements **R_{55} , T_{555} , U_{5555}**



D. Douglas

Non-linear compression

- ❖ JLab IR/UV Upgrade FEL operates with bunch compression ratio of **90-135** (cathode to wiggler); 17-25 (LINAC entrance to wiggler).
- ❖ To achieve this **nonlinear compression** is used compensating for LINAC RF curvature (up to 2nd order)
- ❖ The RF curvature compensation is made **with multipoles** installed in dispersive locations of 180° Bates bend (no harmonic RF used)
- ❖ Operationally longitudinal match relies on:
 1. Bunch length measurements at full compression (modified Martin-Puplett Interferometer)
 2. Longitudinal transfer function measurements **R_{55} , T_{555} , U_{5555}**

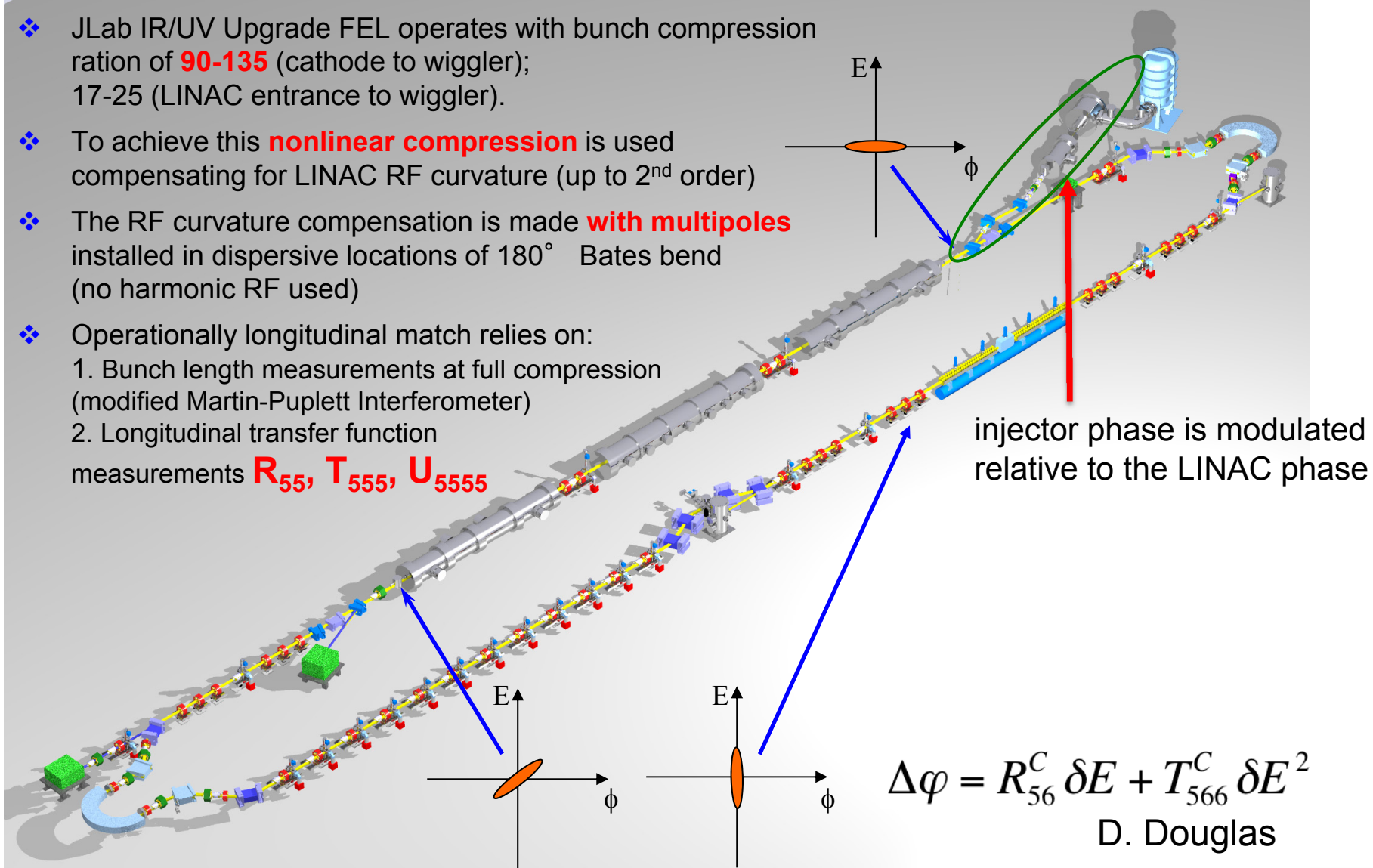


$$\Delta\varphi = R_{56}^C \delta E + T_{566}^C \delta E^2$$

D. Douglas

Non-linear compression

- ❖ JLab IR/UV Upgrade FEL operates with bunch compression ratio of **90-135** (cathode to wiggler); 17-25 (LINAC entrance to wiggler).
- ❖ To achieve this **nonlinear compression** is used compensating for LINAC RF curvature (up to 2nd order)
- ❖ The RF curvature compensation is made **with multipoles** installed in dispersive locations of 180° Bates bend (no harmonic RF used)
- ❖ Operationally longitudinal match relies on:
 1. Bunch length measurements at full compression (modified Martin-Puplett Interferometer)
 2. Longitudinal transfer function measurements **R_{55} , T_{555} , U_{5555}**

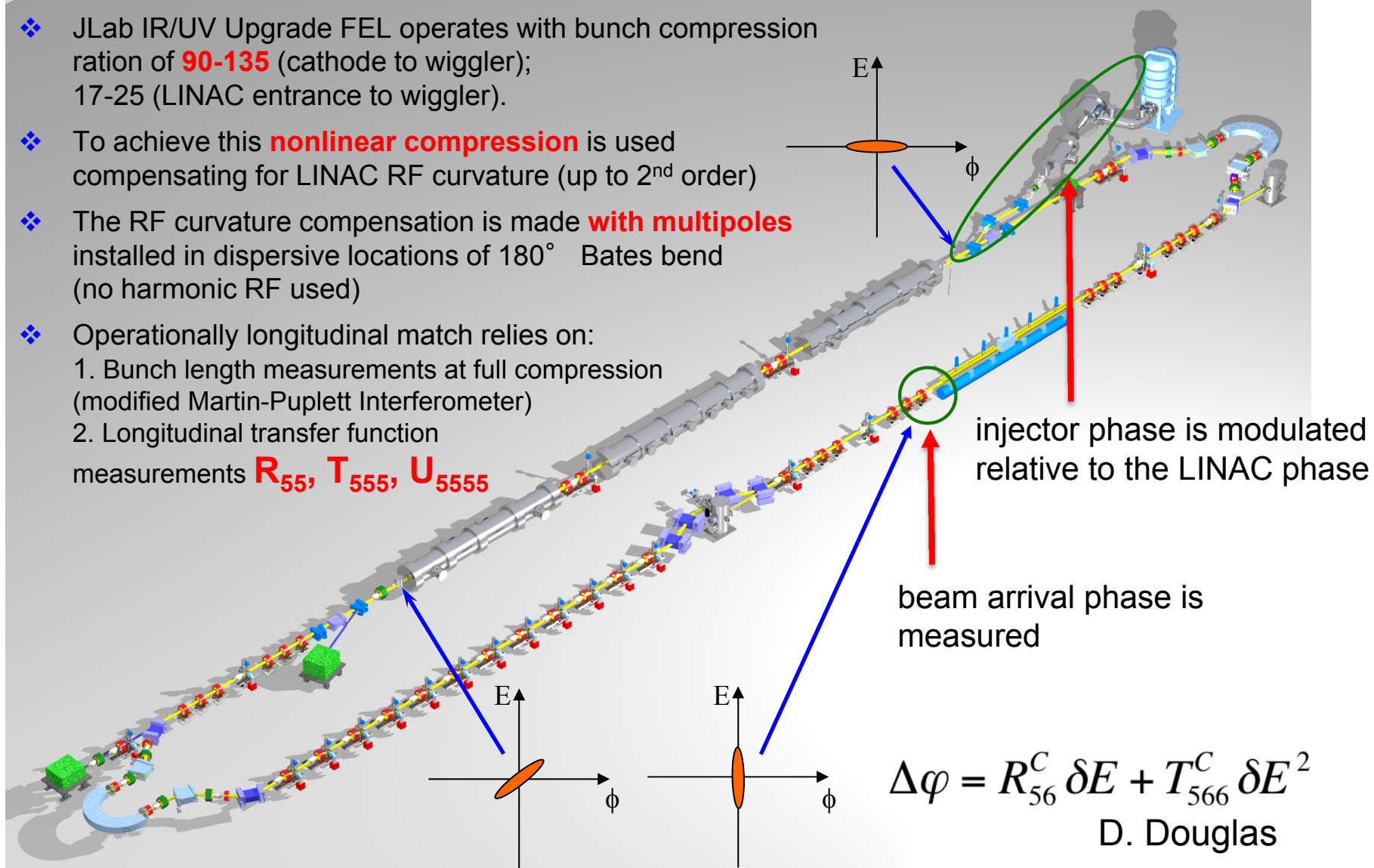


$$\Delta\varphi = R_{56}^C \delta E + T_{566}^C \delta E^2$$

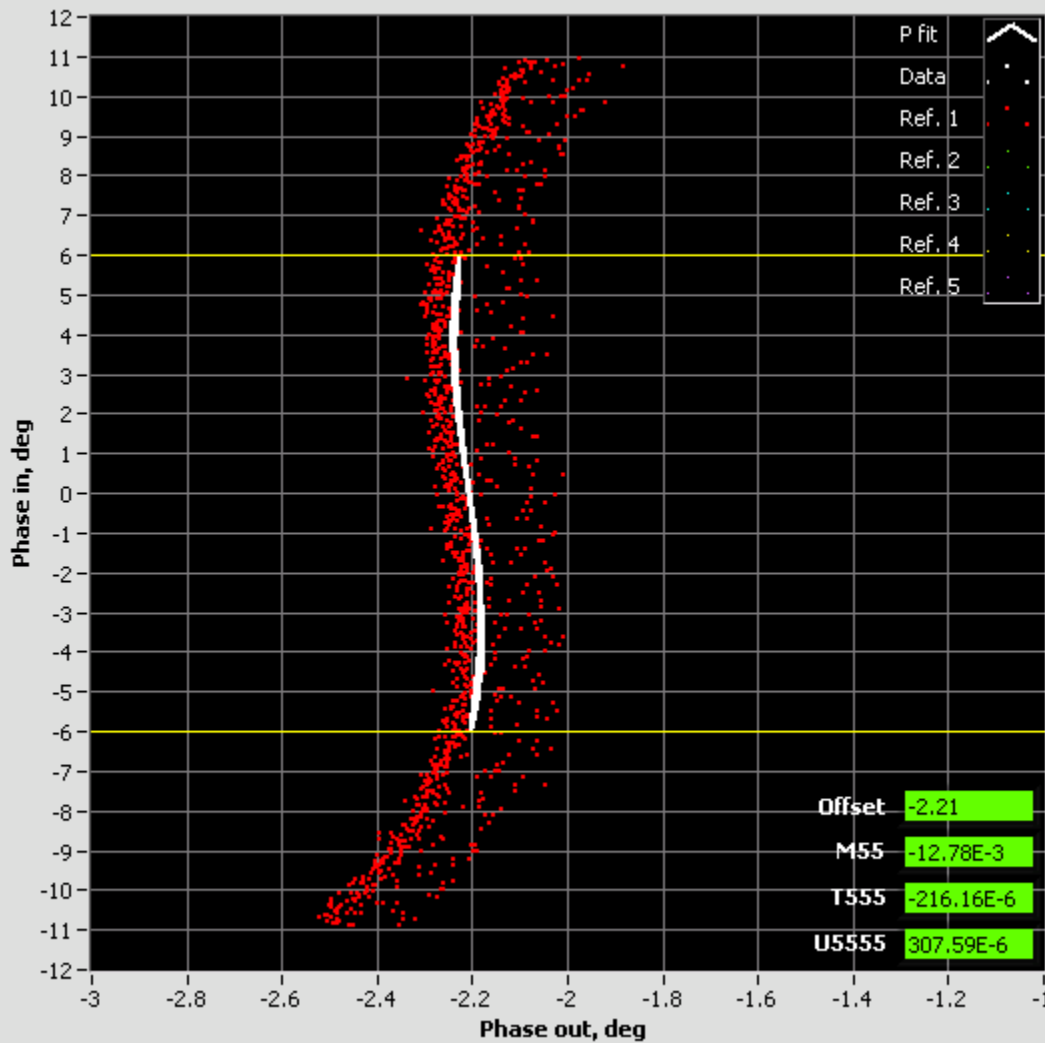
D. Douglas

Non-linear compression

- ❖ JLab IR/UV Upgrade FEL operates with bunch compression ratio of **90-135** (cathode to wiggler); 17-25 (LINAC entrance to wiggler).
- ❖ To achieve this **nonlinear compression** is used compensating for LINAC RF curvature (up to 2nd order)
- ❖ The RF curvature compensation is made **with multipoles** installed in dispersive locations of 180° Bates bend (no harmonic RF used)
- ❖ Operationally longitudinal match relies on:
 1. Bunch length measurements at full compression (modified Martin-Puplett Interferometer)
 2. Longitudinal transfer function measurements **R_{55} , T_{555} , U_{5555}**

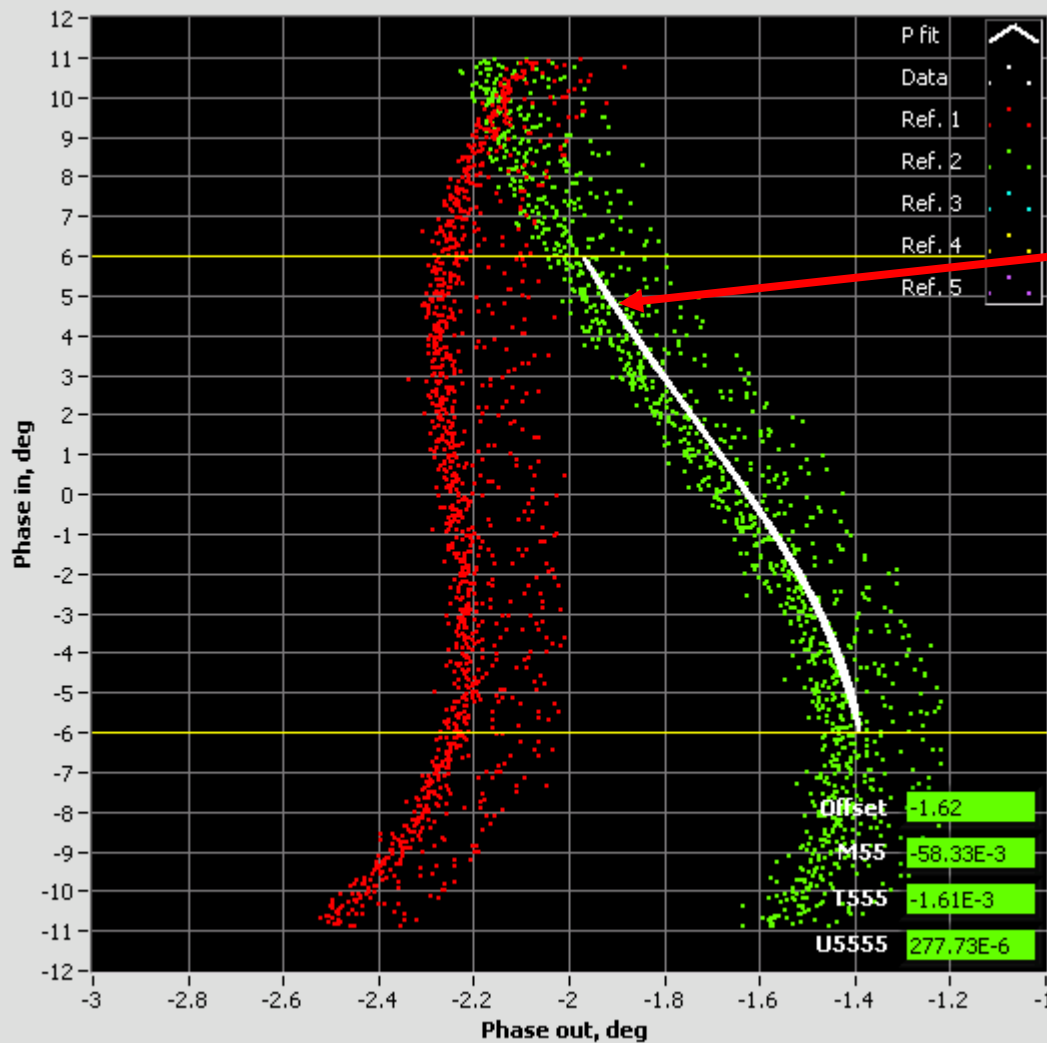


M₅₅ measurements vs. quads



Trim quads – nominal set point of 700 G

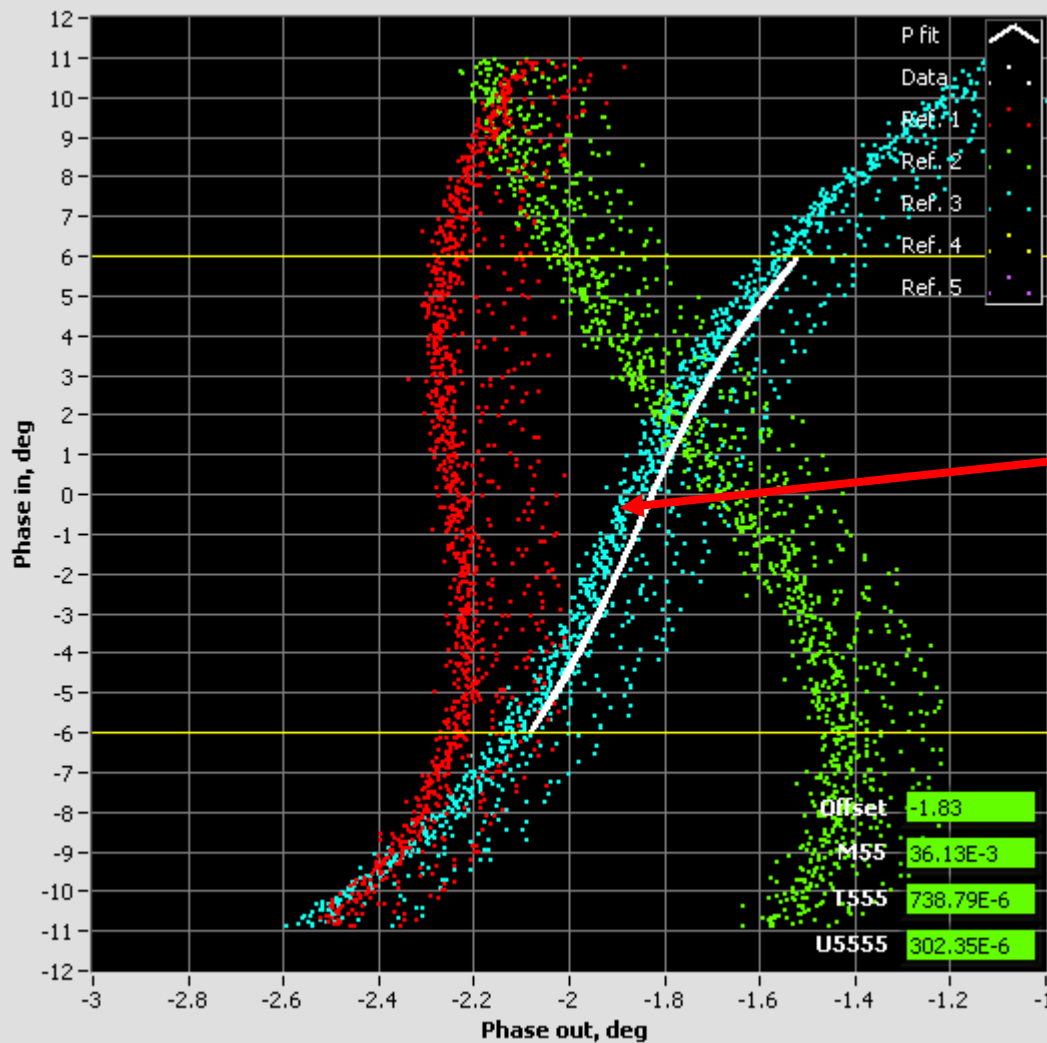
M₅₅ measurements vs. quads



Trim quads – nominal set point of 700 G

Trim quads set point – nominal + 40 G (~ 5.7%)

M₅₅ measurements vs. quads

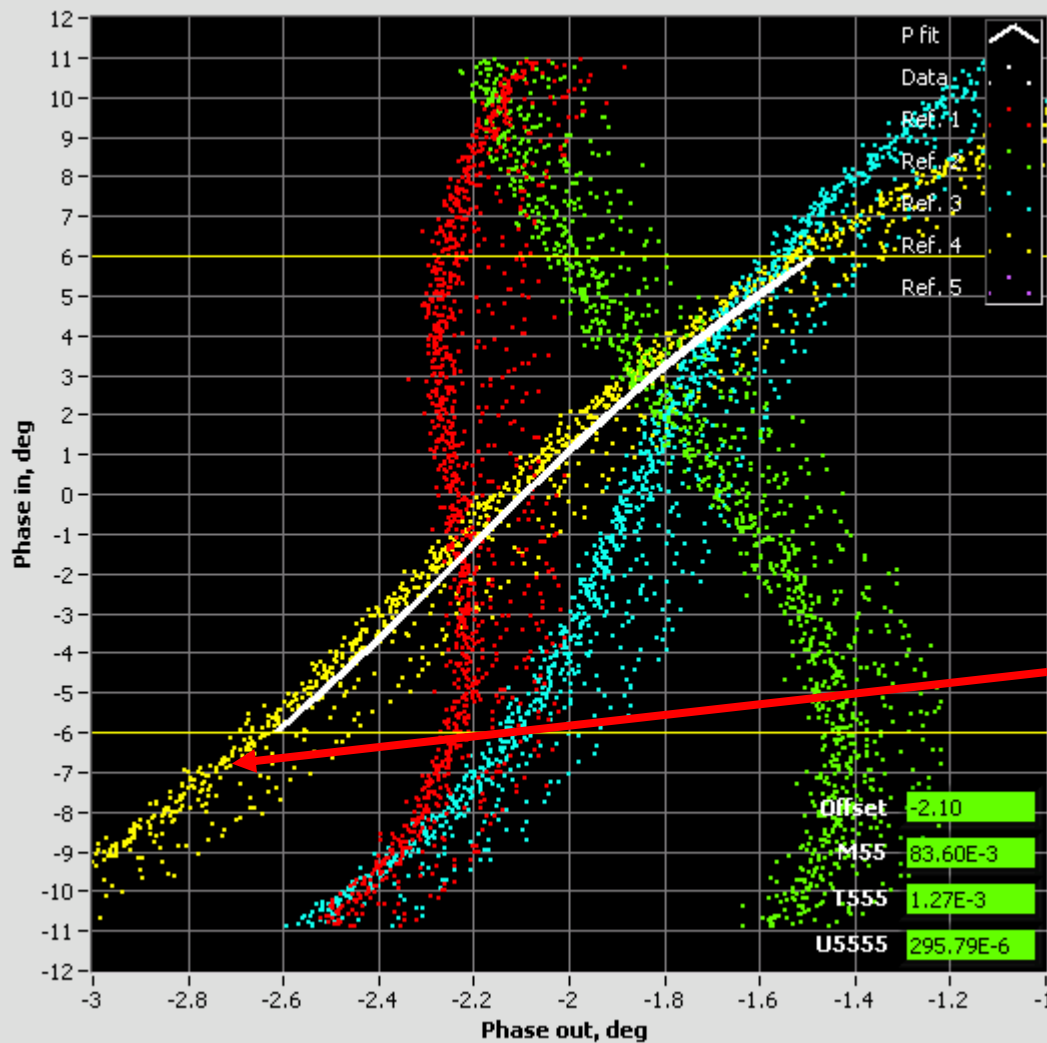


Trim quads – nominal set point of 700 G

Trim quads set point – nominal + 40 G (~ 5.7%)

Trim quads set point – nominal - 40 G (~ 5.7%)

M₅₅ measurements vs. quads



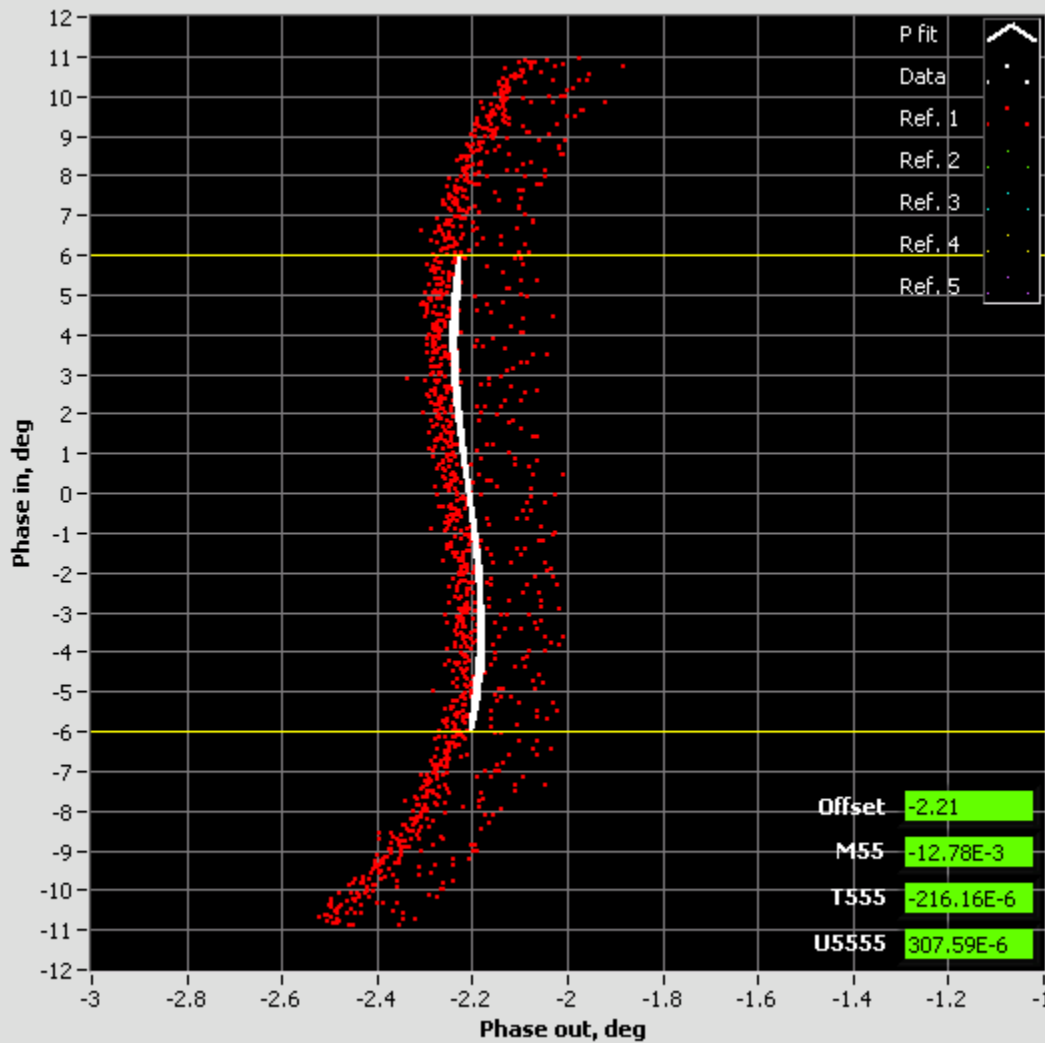
Trim quads – nominal set point of 700 G

Trim quads set point – nominal + 40 G (~ 5.7%)

Trim quads set point – nominal - 40 G (~ 5.7%)

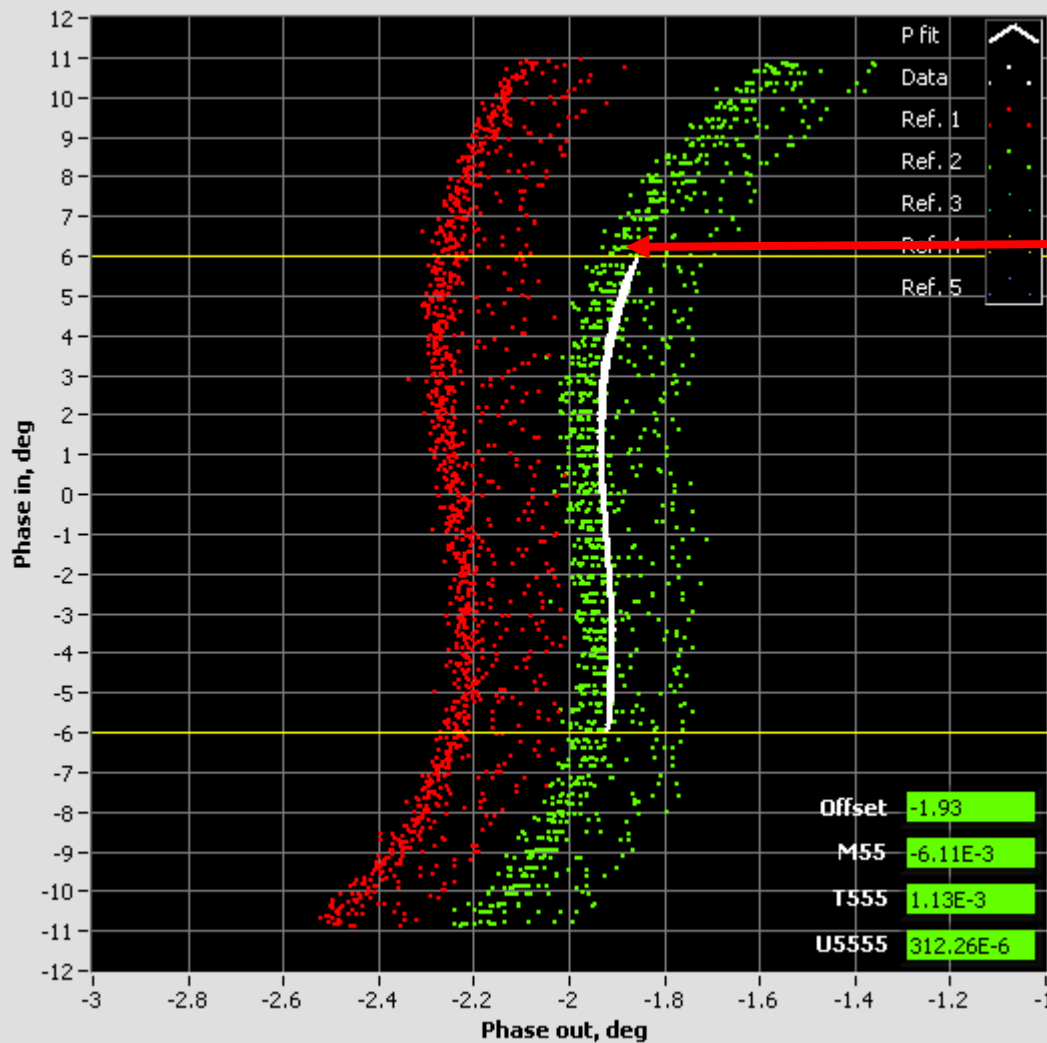
Trim quads set point – nominal - 80 G (~ 11.4%)

M_{55} measurements vs. sextupoles



ARC1 sextupoles nominal
set point 10730 G

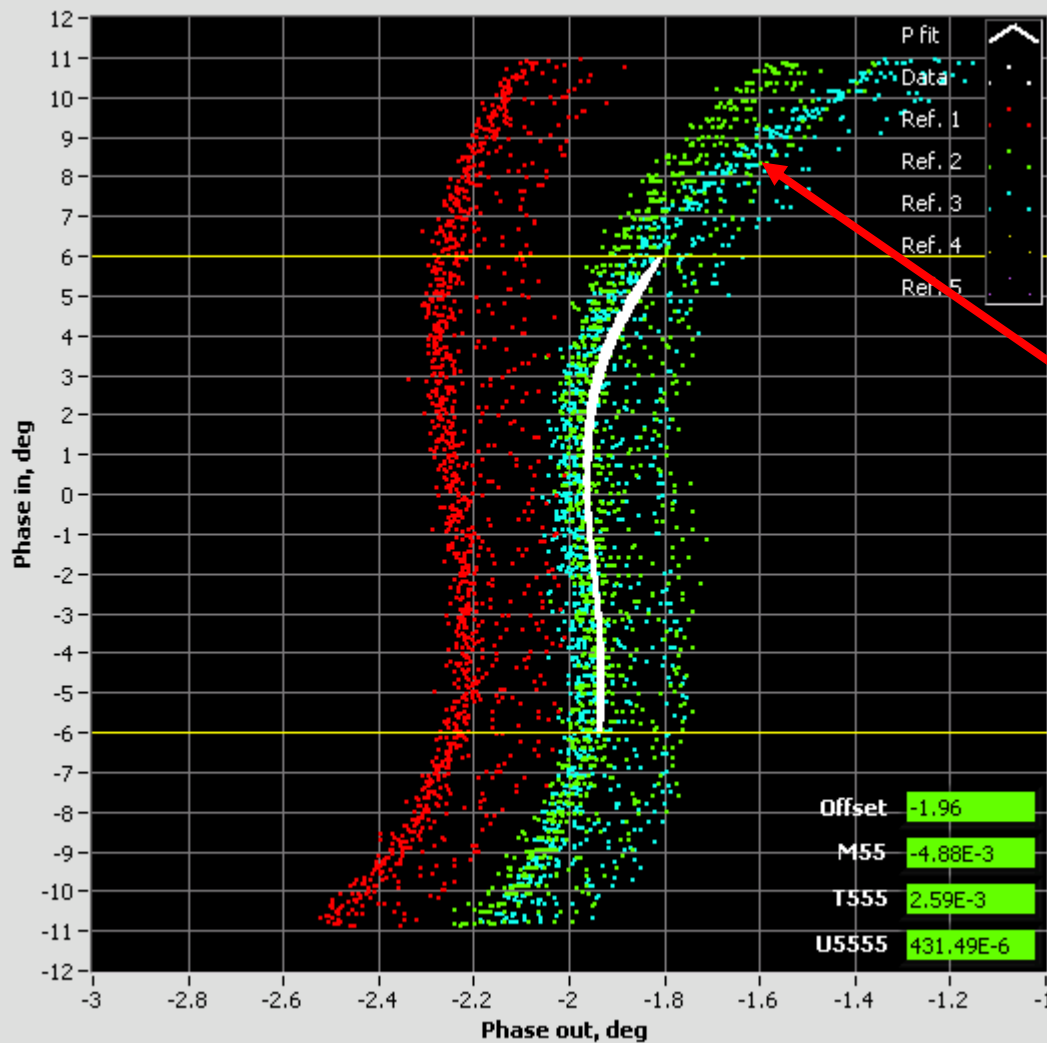
M₅₅ measurements vs. sextupoles



ARC1 sextupoles nominal set point 10730 G

ARC1 sextupoles nominal set point +500 G (~ 4.7 %)

M₅₅ measurements vs. sextupoles

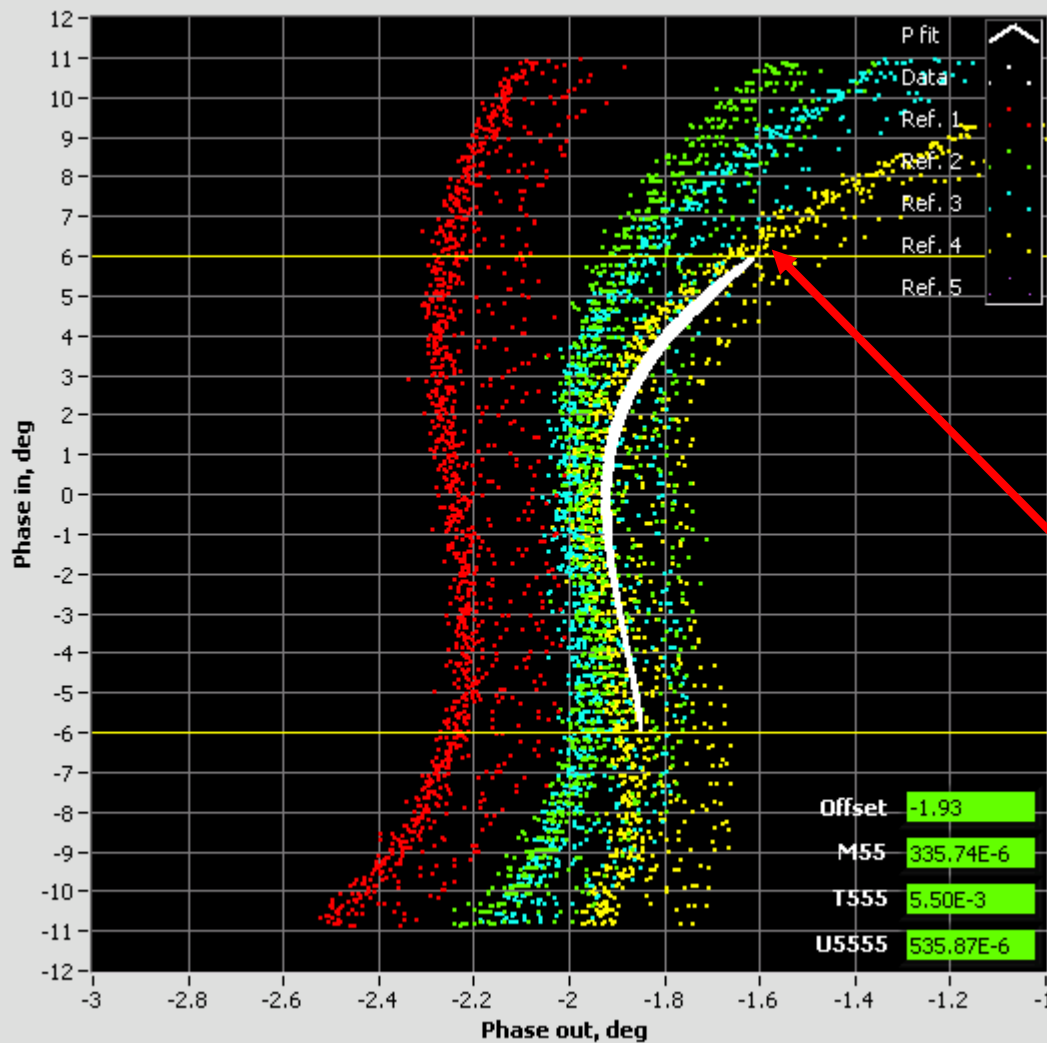


ARC1 sextupoles nominal
set point 10730 G

ARC1 sextupoles nominal
set point +500 G (~ 4.7 %)

ARC1 sextupoles nominal
set point +1000 G

M_{55} measurements vs. sextupoles



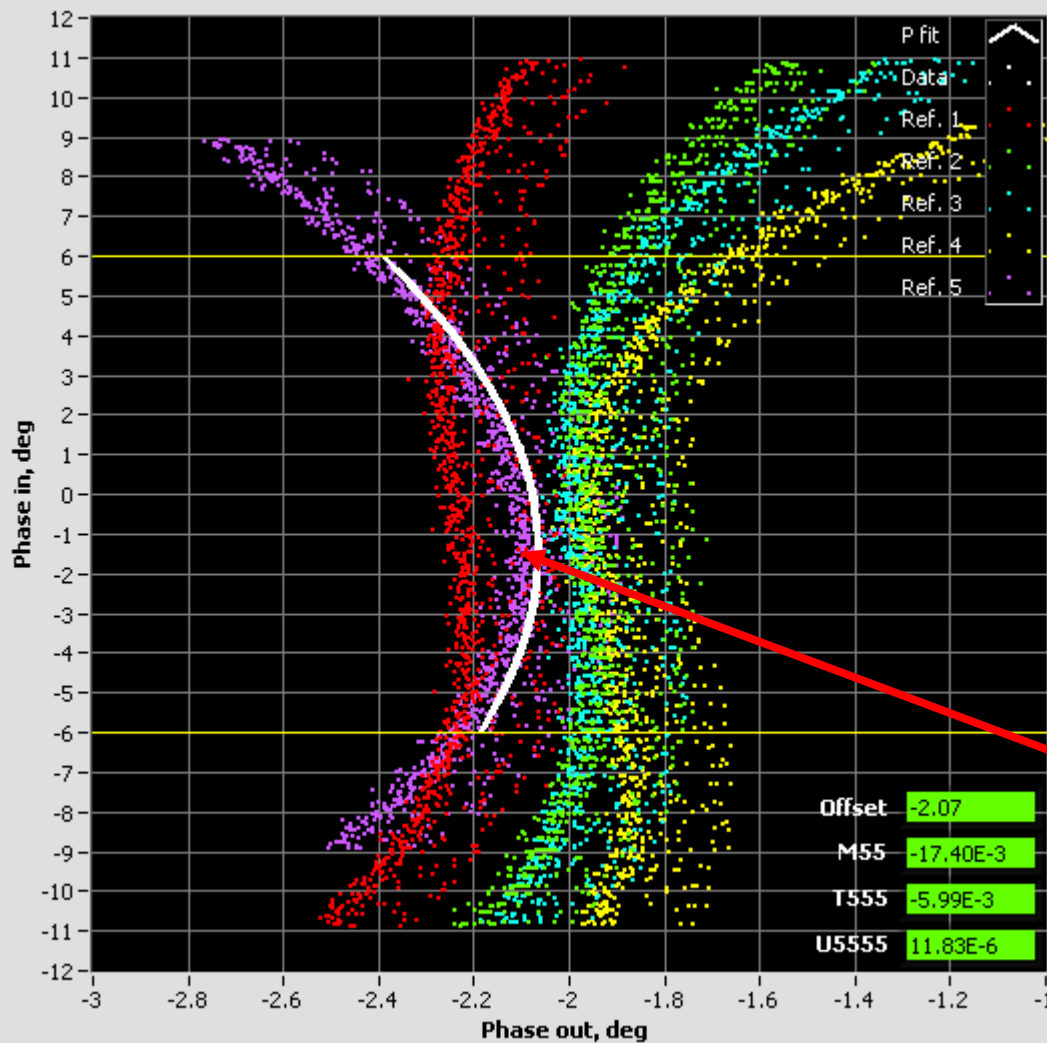
ARC1 sextupoles nominal
set point 10730 G

ARC1 sextupoles nominal
set point +500 G (~ 4.7 %)

ARC1 sextupoles nominal
set point +1000 G

ARC1 sextupoles nominal
set point +2000 G

M₅₅ measurements vs. sextupoles



ARC1 sextupoles nominal
set point 10730 G

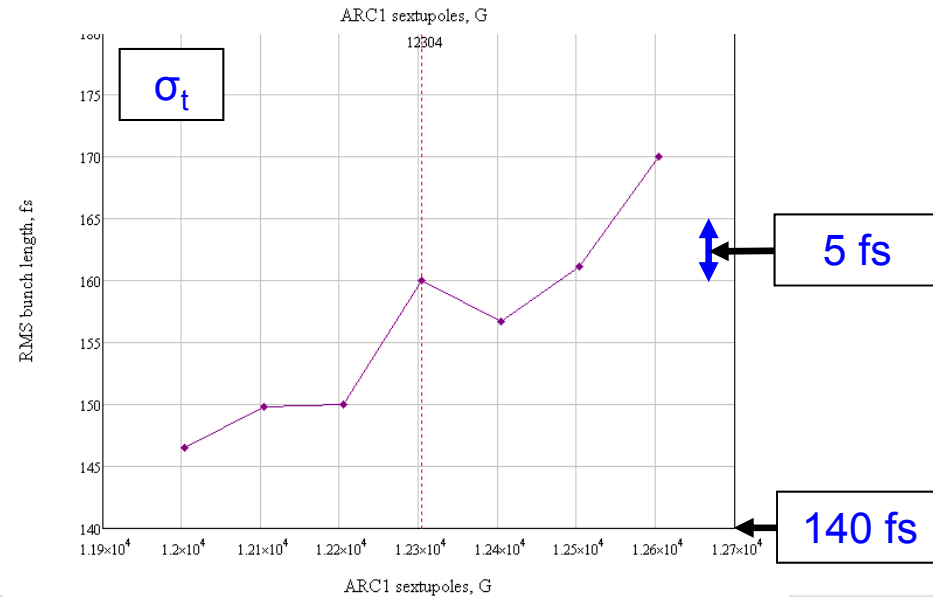
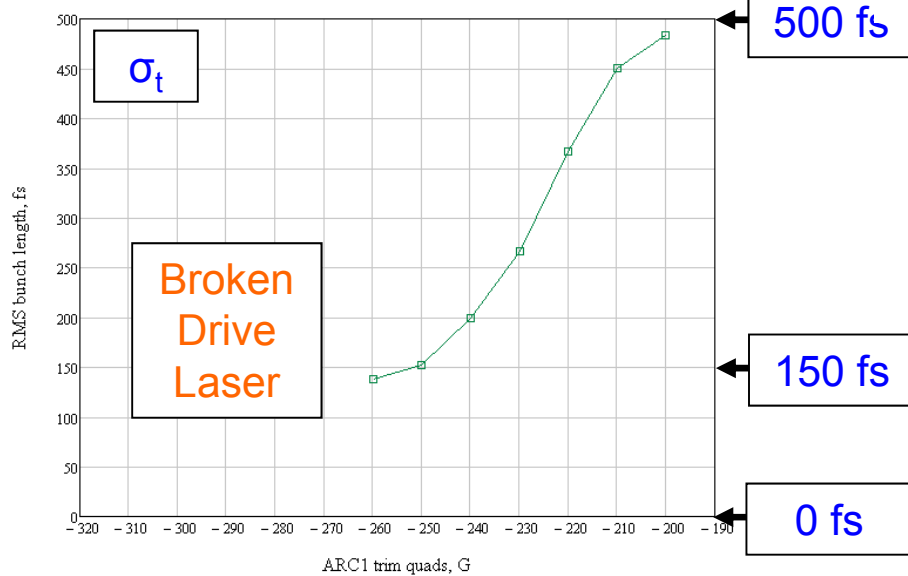
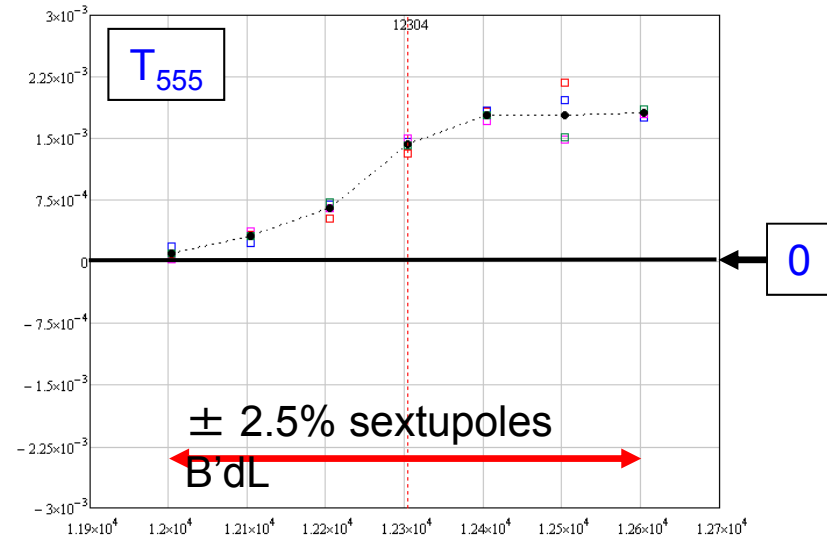
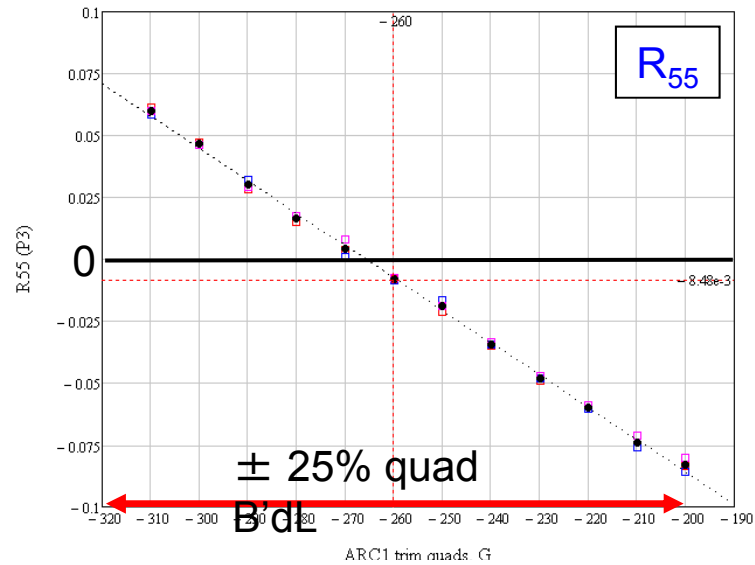
ARC1 sextupoles nominal
set point +500 G (~ 4.7 %)

ARC1 sextupoles nominal
set point +1000 G

ARC1 sextupoles nominal
set point +2000 G

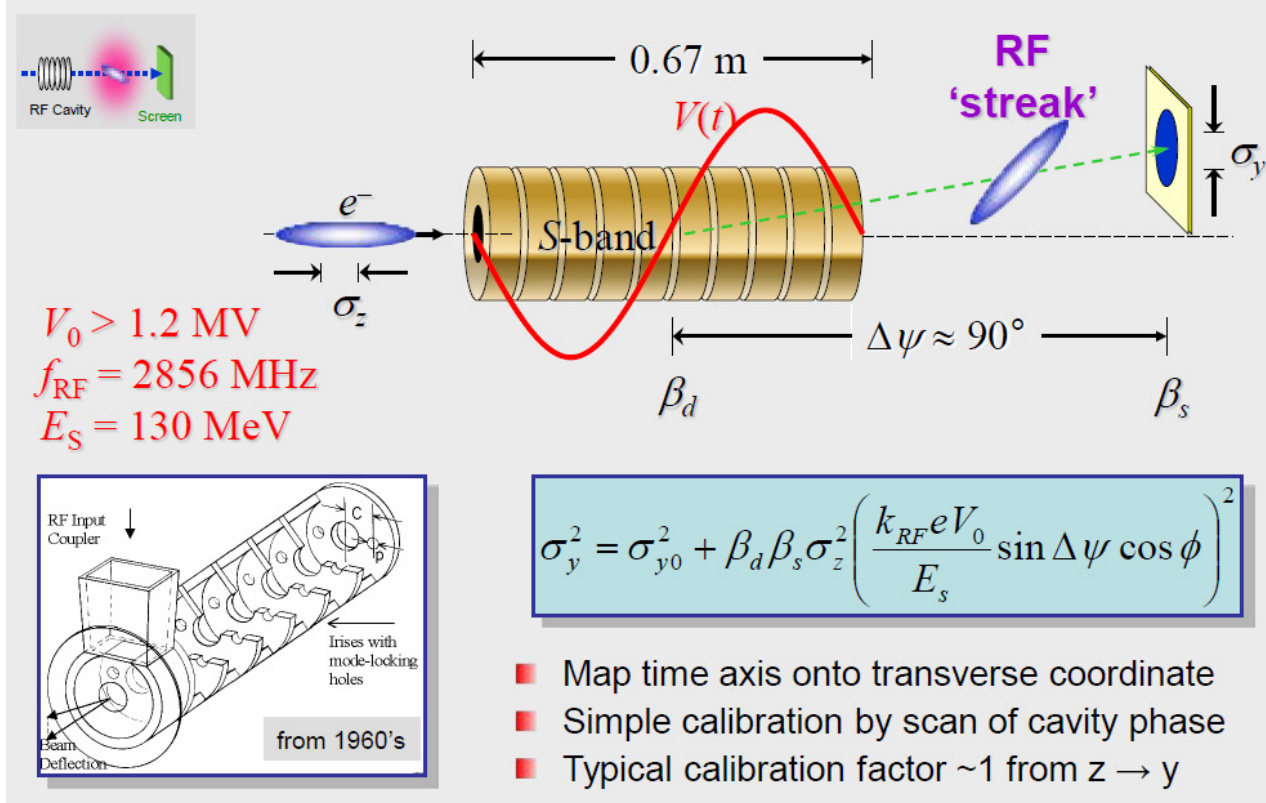
ARC1 sextupoles nominal
set point -2000 G

Bunch length - M_{55} – trim quads



Transverse deflecting cavity (TCAV)

Courtesy of
P. Krejcik & Y. Ding



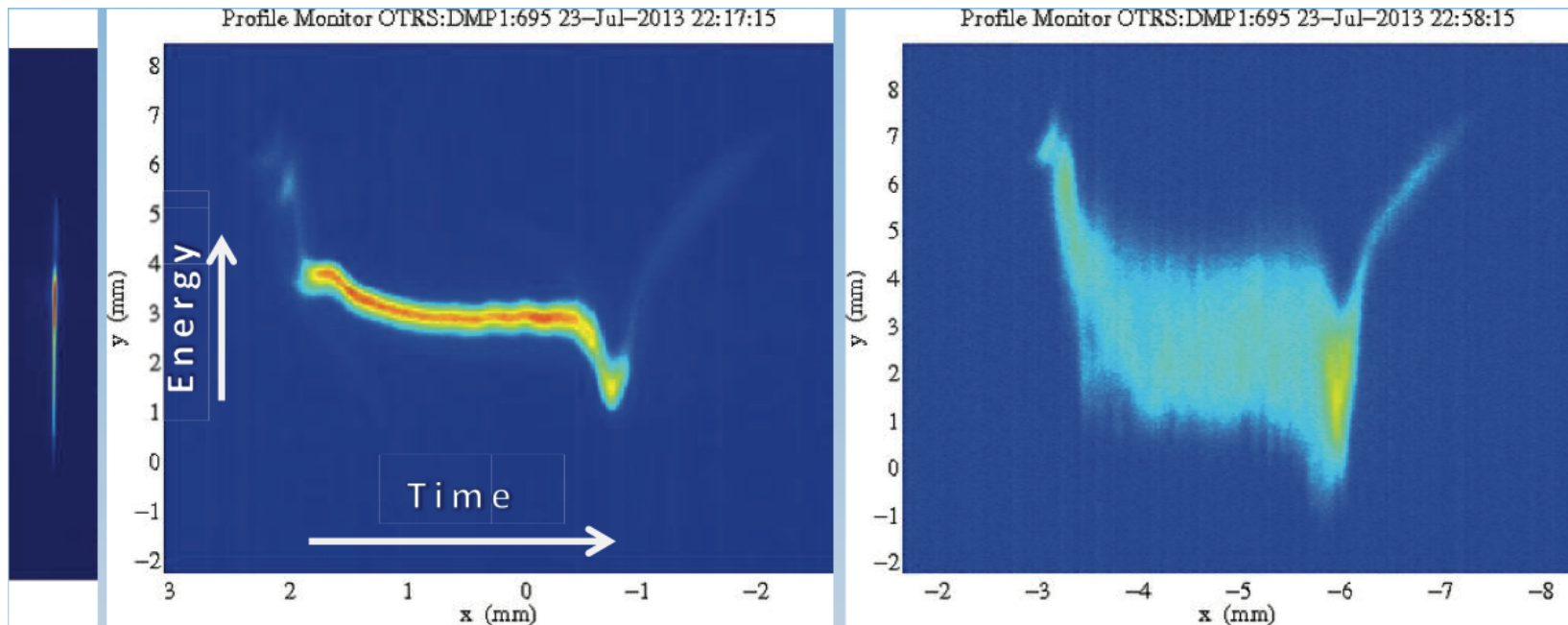
- ❖ Transverse deflecting cavity “gold standard”; direct, time domain, self calibrating measurements
- ❖ At LCLS bunch length shorter than could be resolved with S-band TCAV
- ❖ Going to X-band \rightarrow 1 fs resolution
- ❖ Provide absolute measurements which can be used to calibrate frequency domain diagnostics
- ❖ Expansive and large complex installations. Not every facility can afford it.

X-band TCAV → XTCAV at LSLC

Courtesy of
P. Krejcik & Y. Ding

XTCAV differs from S-band TCAV in three important respects

- ❖ Operates at 11.424 GHz; over all improvement of time resolution x8 (x4 from frequency and x2 from field amplitude)
- ❖ Installed downstream of the LCLS undulator, does not interfere with FEL operation, operates at full rep. rate of 120 Hz
- ❖ Not only e- beam diagnostic but also X-ray temporal profile measurements and FEL interaction efficiency

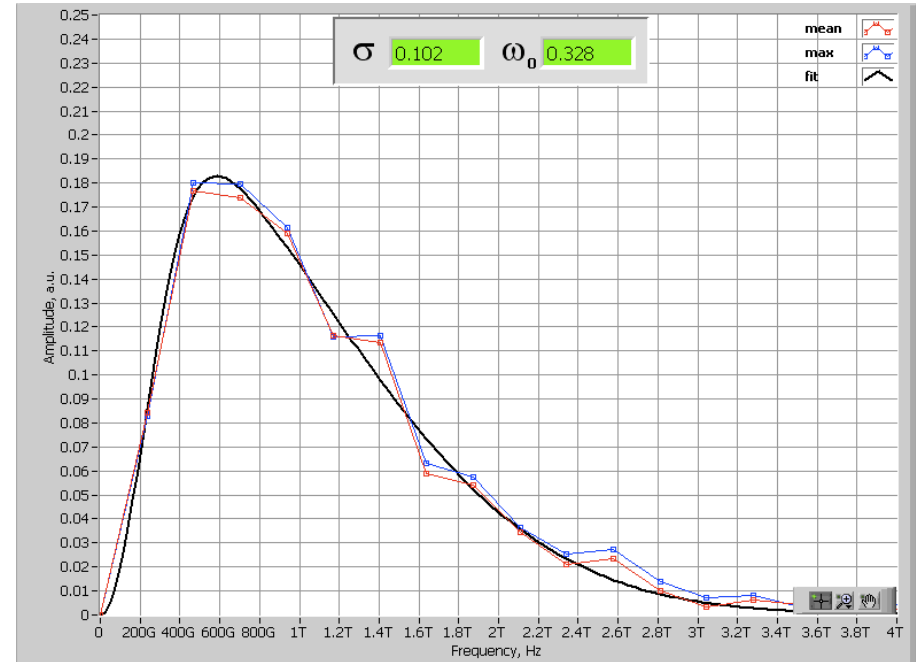
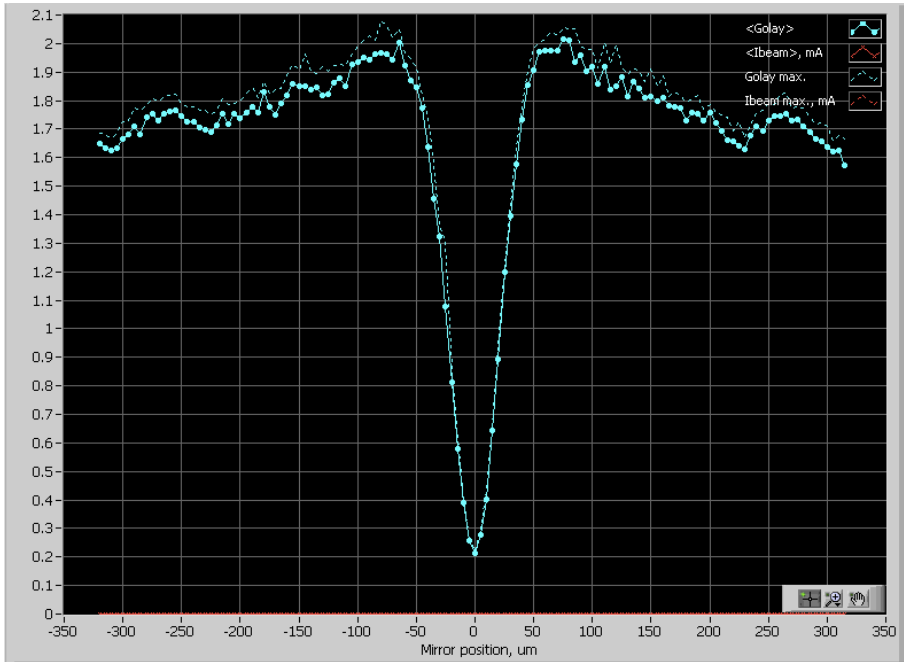


XTCAV **off**

XTCAV **on** FEL **off**

XTCAV **on** FEL **on**

Bunch length via frequency domain

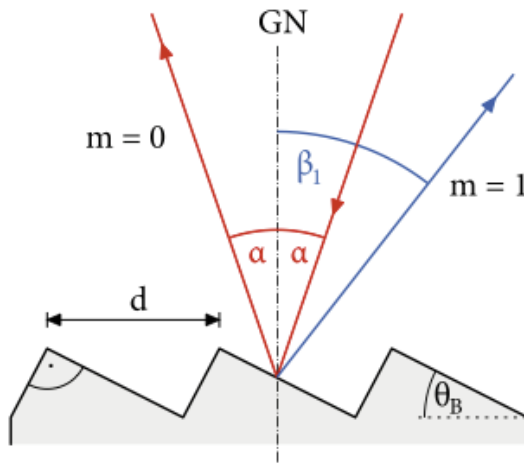


- ❖ Martin-Puplett interferometer or FTIR
- ❖ measures autocorrelation function of CTR or CSR
- ❖ Power spectrum is Fourier transform of the autocorrelation
- ❖ phase information is not measured
- ❖ multi-shot measurements; still can be very fast with CW beam and FTIR-like

Reflective blazed gratings

- ▶ Polarisation \perp groove
- ▶ Blaze angle $\theta_B = 27^\circ$
- ▶ Incident angle $\alpha = 19^\circ$

$$m \frac{\lambda}{d} = \sin(\alpha) + \sin(\beta)$$

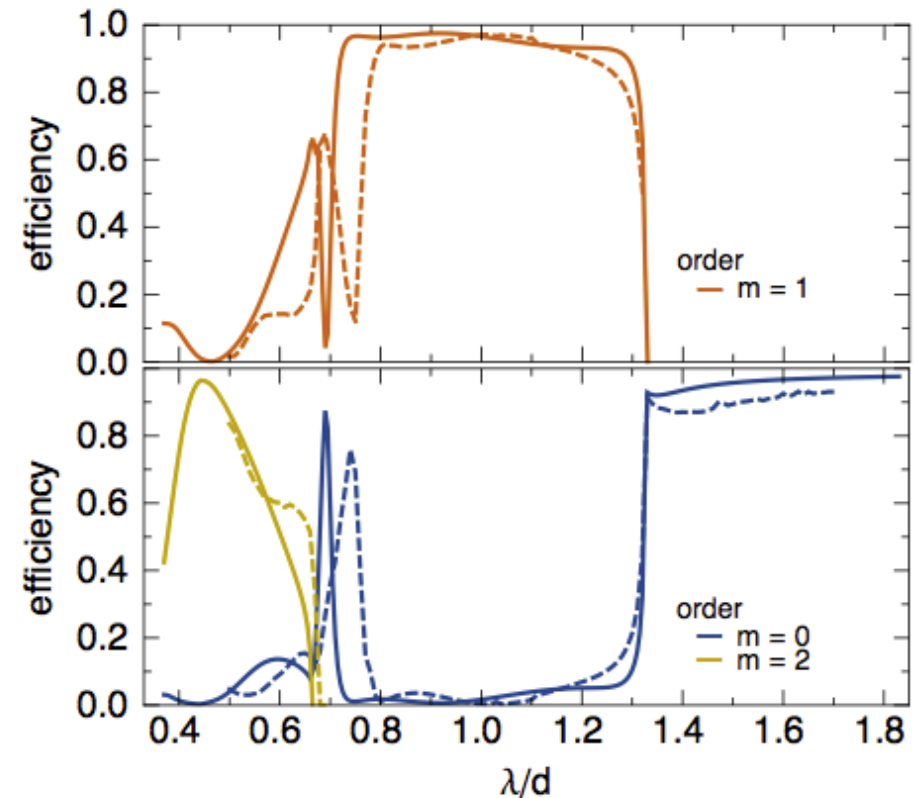


E. Hass, B. Schmidt and S. Wesch



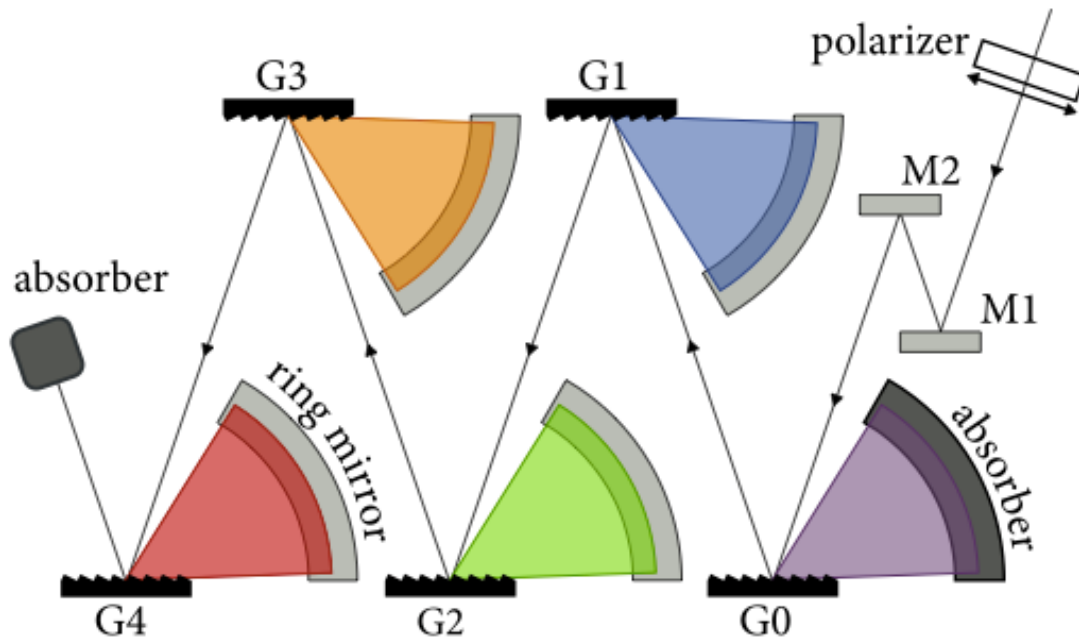
A multi-channel THz and infrared spectrometer for femtosecond electron bunch diagnostics by single-shot spectroscopy of coherent radiation

Stephan Wesch*, Bernhard Schmidt, Christopher Behrens, Hossein Delsim-Hashemi, Peter Schmüser

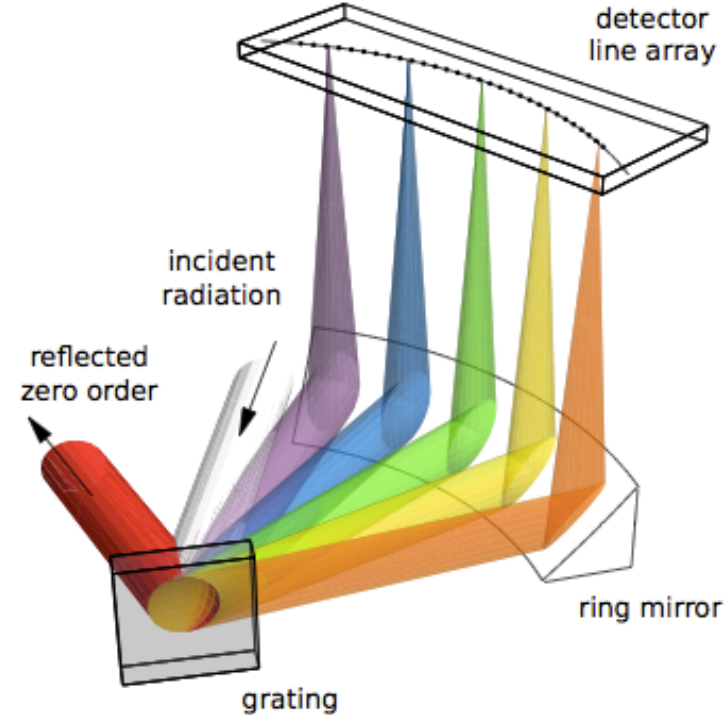


Staged spectrometer

Each stage acts as dispersive element
+ filter for next stage



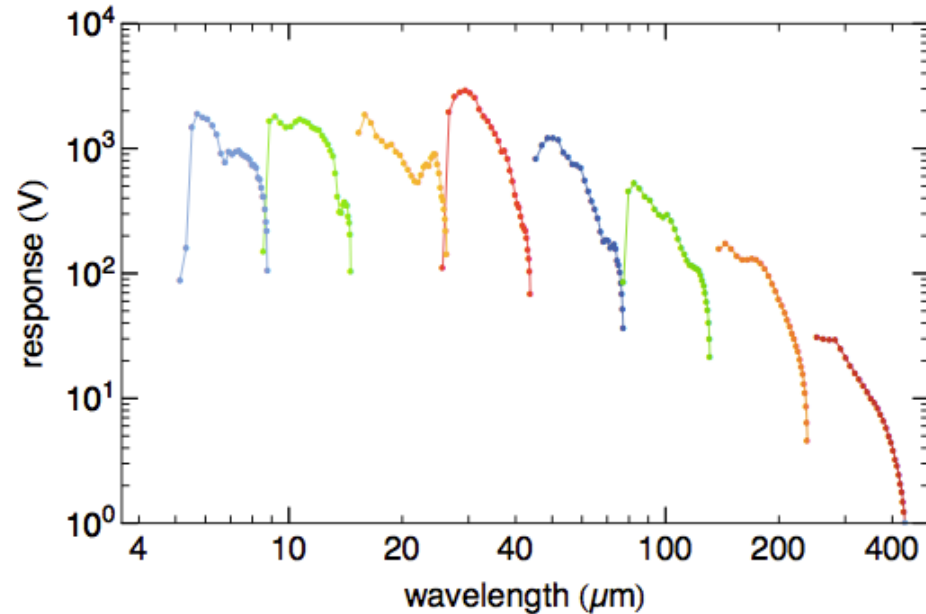
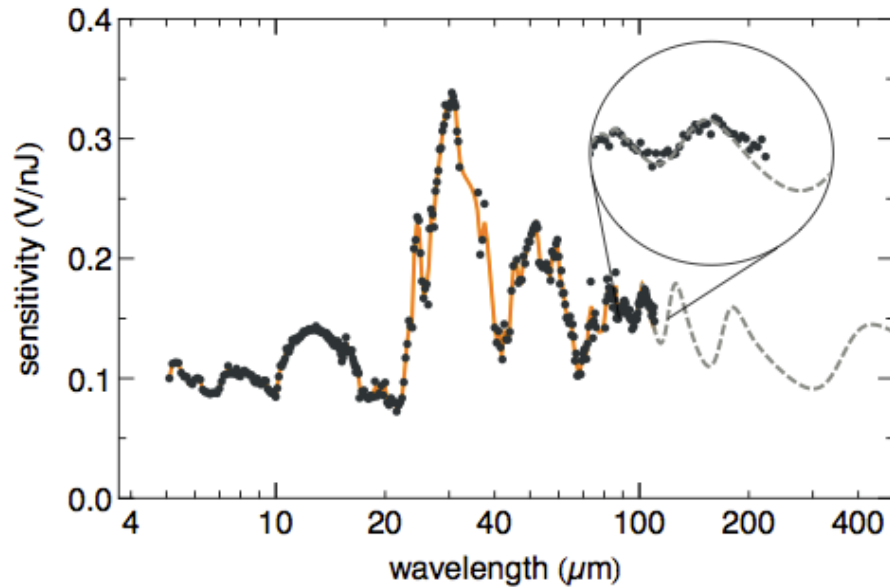
- ❖ each grating covers λ range of about 2
- ❖ one set of 4 gratings covers factor of 10
- ❖ two sets of gratings



- ▶ Parallel readout
- ▶ 4 Stages cover one order of magnitude in λ

E. Hass, B. Schmidt and S. Wesch

CRISP4 absolute calibration



Pyro-electric detector absolute calibration

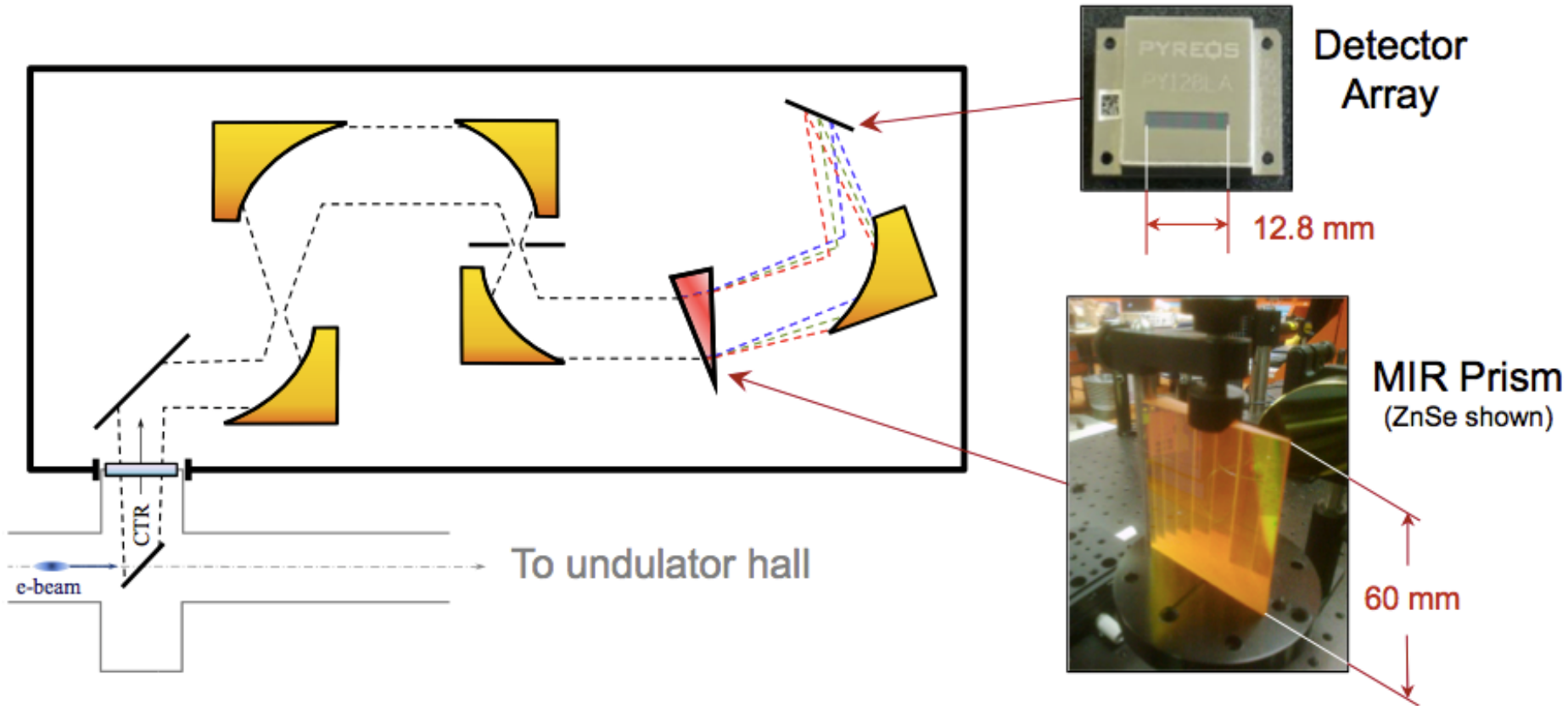
- ❖ MIR region calibrated at FELIX
- ❖ FIR region modeled
- ❖ The model describes FIR and partially MIR where it is benchmarked by the measurements

Complete calibration of the spectrometer

- ❖ CTR source
- ❖ Transport from source to detector(s)
- ❖ Gratings efficiency
- ❖ Detector (as shown to the left)
- ❖ Electronics

E. Hass, B. Schmidt and S. Wesch

MIR prism spectrometer



- Prism: 10° apex, KRS-5 ($T = 0.6 - 40 \mu\text{m}$) or ZnSe ($T = 0.5 - 20 \mu\text{m}$)
- Detector: Linear PZT pyroelectric array, 100 μm pitch

T. Maxwell, H. Loos, Y. Ding

Prism spectrometer response

Amplitude Response $T(\kappa)$

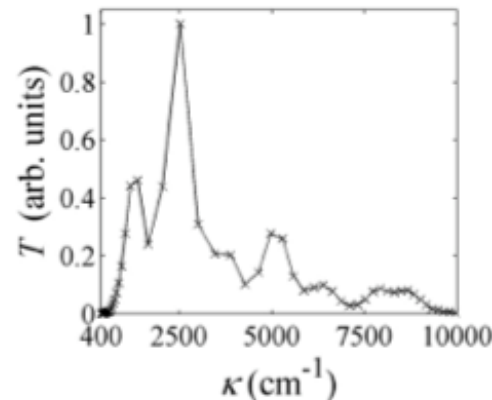
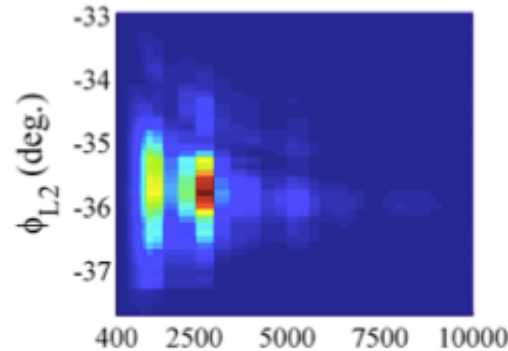
$$I[x(\kappa)] \approx \left[\frac{d\kappa}{dx} \right] T_{\text{det}}(\kappa) T_{\text{abs}}(\kappa) I_e(\kappa) |f(\kappa)|^2$$
$$= T(\kappa) |f(\kappa)|^2$$

1. Recon. $T(\kappa)$ by varying κ -independent param (ϕ_{L2})
2. Compare to *LiTrack* simulated ϕ_{L2} scans

$$I(\kappa; \phi_{L2}) = T(\kappa) |f(\kappa; \phi_{L2})|^2$$

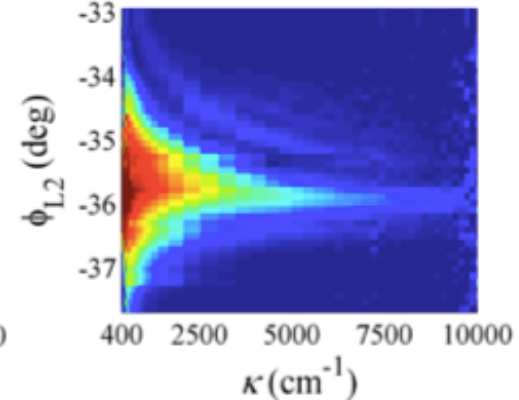
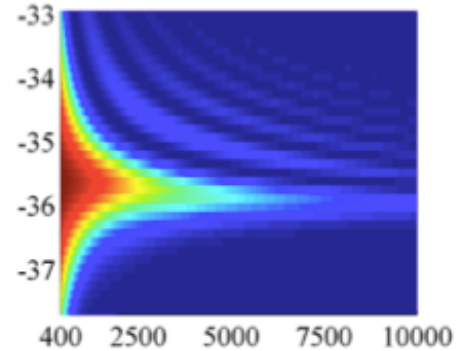
3. Fit missing $T(\kappa)$ (and machine parameters)

1) Measured Spectra*



3) Instrument Resp.

2) Simulated Spectra



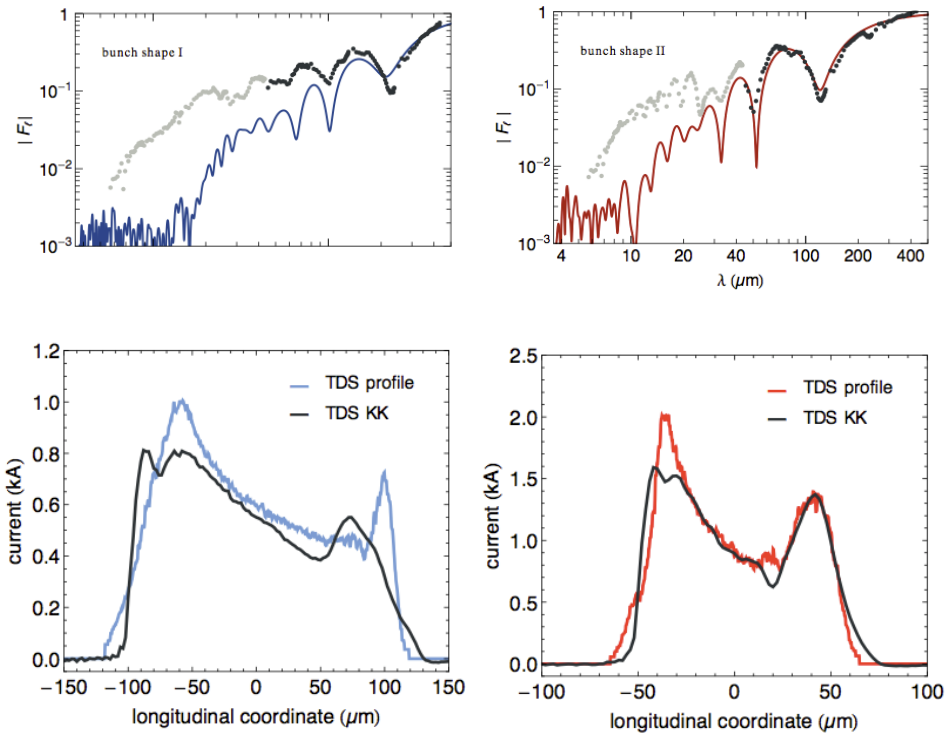
4) Corrected Measurement

T. Maxwell, H. Loos, Y. Ding

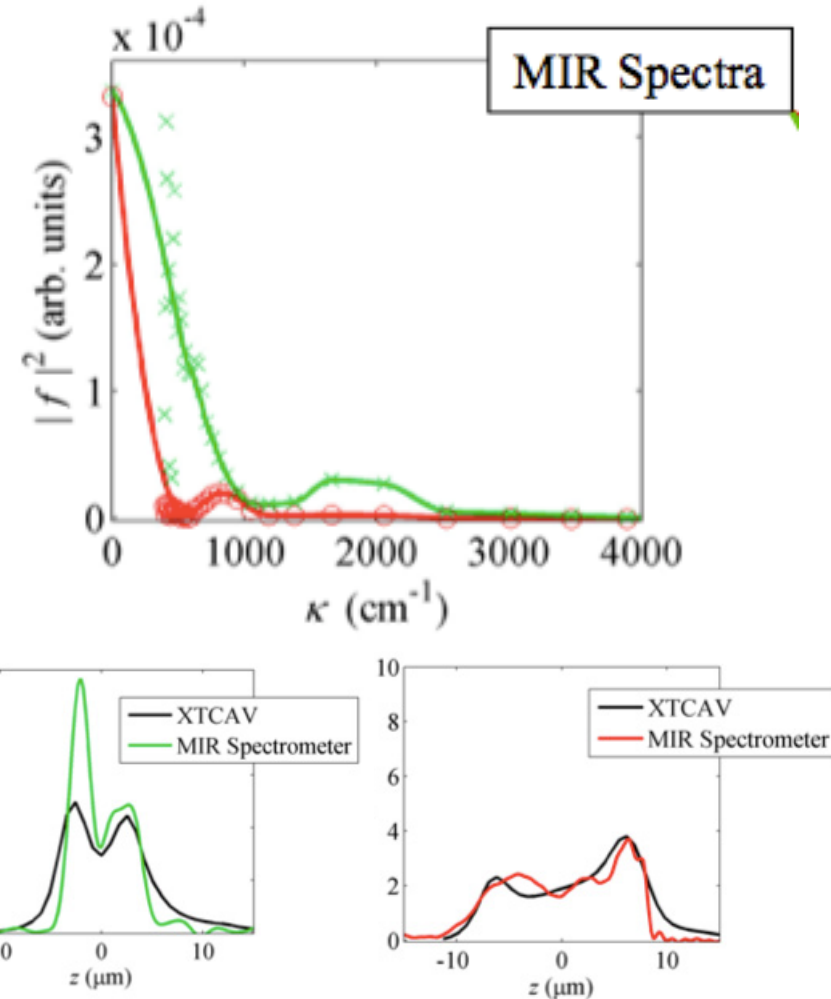
Longitudinal distribution reconstruction

Grating spectrometer

Comparing to Transverse Deflecting Structure measurements in both frequency domain and time domain



Prism spectrometer



In conclusion

- ❖ The need for beam diagnostics for FEL drivers that are beyond standard ones is much larger than presented here, which was a subjective and based choice. *Apologies if your favorite problem of diagnostic was not mentioned.*
- ❖ One of the directions new for X-ray FELs, but previously explored with IR FELs is operation with CW beam and average current many orders of magnitude larger than used presently by X-ray FELs. *It is suggested, that diagnostics with much larger dynamic range are needed to address this challenge.*
- ❖ Another challenging frontier is the extremely short bunch length; *on the order of few fs*
- ❖ Impressive time- and frequency- domain instruments have been already developed; resolution on the order of fs. *Yet, both have their own cons: cost and complexity (time domain), lost phase information (frequency domain)*

Thank you.